Doppler effects in heterogeneous media with applications to ocean acoustic modeling

Peter B. Weichman
BAE Systems, Advanced Information Technologies, 6 New England Executive Park, Burlington, Massachusetts 01803, USA
(Received 25 January 2005; revised manuscript received 9 September 2005; published 6 December 2005)

Doppler shift corrections to ocean acoustic signals are complicated by the multi-spatial-scale structure of the ocean medium, resulting in a multi-time-scale structure of the acoustic Green function. Repeated reflections and refractions lead in general to an infinite number of acoustic paths or modes, with different times of flight, connecting source and receiver. The rate of change of these flight times with source or receiver motion gives rise to Doppler shift corrections, and each acoustic path or mode has a *different* correction. A clean Doppler correction (in the sense of an observable coherent motion-induced frequency shift for each path or mode) is shown to emerge only when the medium is homogeneous *along* the direction of source or receiver motion, even when it is highly inhomogeneous in directions orthogonal to the motion. A very general quantitative theory for this correction is developed, encompassing earlier results in the literature, and presented in a form amenable to efficient numerical implementation in data processing.

DOI: 10.1103/PhysRevE.72.066602 PACS number(s): 43.30.+m, 43.20.+g, 43.58.+z, 92.10.Vz

I. INTRODUCTION

The classic Doppler frequency shift $\omega=\omega_0+\Delta\omega$ for a harmonic source with angular frequency ω_0 moving in an infinite homogeneous acoustic medium with sound speed c is given by

$$\frac{\Delta\omega}{\omega_0}=\frac{\hat{\mathbf{n}}_{rs}\cdot(\mathbf{v}_s-\mathbf{v}_r)/c}{1-\hat{\mathbf{n}}_{rs}\cdot\mathbf{v}_s/c}, \tag{1.1}$$

where $\mathbf{v}_s$ and $\mathbf{v}_r$ are, respectively, the source and receiver velocities—see Fig. 1. To lowest order in v/c, where v represents the overall scale of $|\mathbf{v}_s|$ and $|\mathbf{v}_r|$, $\hat{\mathbf{n}}_{rs}(t)$ is the (instantaneous) unit vector pointing from source position $\mathbf{x}_s(t)$ to receiver position $\mathbf{x}_r(t)$. Higher order corrections arise from propagation delay effects: in fact $\hat{\mathbf{n}}_{rs}$ should point from where the source was at the retarded time t', when the signal left the source, determined by the condition $t-t'=|\mathbf{x}_r(t)-\mathbf{x}_s(t')|/c$. The formula (1.1) also remains valid for accelerating source and receiver if one interprets $\mathbf{v}_r=\dot{\mathbf{x}}_r(t)$, $\mathbf{v}_s=\dot{\mathbf{x}}_s(t')$, the instantaneous velocities at actual and retarded times. Since the measurement of a well defined frequency to an accuracy $\Delta\omega$ requires observation of a stable harmonic signal over a time interval Δt of order $2\pi/\Delta\omega$, implicit in Eq. (1.1) is the assumption that time variation of the right hand side be slow on this same scale. This places limits on both source and receiver speed (through the rates of change of both the cross range $\hat{\mathbf{n}}_{rs}$ and the range $|\mathbf{x}_r-\mathbf{x}_s|$, since the latter determines the overall amplitude of the signal) and acceleration. The former requires that

$$\frac{\lambda}{|\mathbf{x}_r-\mathbf{x}_s|}\ll 1, \tag{1.2}$$

where $\lambda=2\pi c/\omega_0$ is the wavelength. This turns out not to be a limit on the velocities, but on the number of wavelengths over which the outgoing wave from the source may be approximated locally by a plane wave: larger v reduces Δt, but increases $\Delta\omega$ in such a way that the product $\Delta\omega\Delta t$ remains unchanged. The condition on the acceleration is

$$\frac{\lambda_0 a}{v^2}\ll 1, \tag{1.3}$$

where a represents the overall scale of $|\dot{\mathbf{v}}_s|$ and $|\dot{\mathbf{v}}_r|$. This may be written in the form $\lambda_0/v\ll v/a$, which states that the time to travel a wavelength should be much smaller than the time over which the velocities change by a factor of order unity.

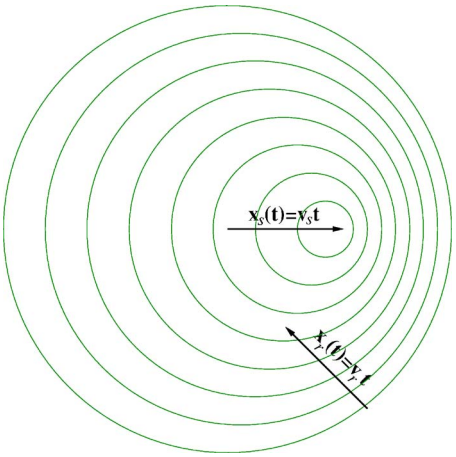

FIG. 1. (Color online) A snapshot of the wave fronts produced by a source with fixed frequency ω_0 moving at a uniform velocity $\mathbf{v}_s$, in this case through a homogeneous medium. The receiver, moving at velocity $\mathbf{v}_r$, sees a Doppler shifted frequency $\omega(t)$ determined by the rate at which it crosses these wave fronts, which must be nearly equally spaced (local plane wave condition) in order for $\omega(t)$ to be well defined. In this case, wave fronts are spherical, and this leads to the condition (1.2) that the source-receiver separation be much larger than the wavelength. For an inhomogeneous medium, the wave fronts will be nonspherical and their local spacing may vary strongly—leading to an ill-defined local wave number. There may, however, be certain symmetry directions, together with a more general condition (1.4), along which they are nearly equally spaced and if $\mathbf{v}_s$ and $\mathbf{v}_r$ conform to these directions, a well defined Doppler frequency will exist.

The aim of this paper is to generalize all of the above notions, to the greatest degree possible, to more complicated acoustic media, bounded by various interfaces, and with sound speed that may vary strongly with position. Examples to keep in mind are deep ocean and littoral environments with depth- and range-dependent sound speed profiles, range-dependent bathymetry, and heterogeneous propagation parameters in the sea bottom.

A few key ideas underlie the results:

(1) The existence of strong reflection and refraction effects in heterogeneous environments implies that a single source will in general produce multiple arriving waves at the receiver. At minimum therefore generalization of the notion of Doppler shift requires a decomposition of the signal into an infinite number of separate arrivals from different directions, each with its own frequency shift [1–4]. Heuristically, a different version of Fig. 1 could be plotted for each arrival.

(2) Generalization of Eq. (1.2) determines the criterion for the existence of a well defined Doppler shift: there must be a length scale ξ (replacing $|\mathbf{x}_r - \mathbf{x}_s|$) with

$$\frac{\lambda}{\xi} \ll 1, \tag{1.4}$$

such that *along both source and receiver trajectory* each arrival component of the acoustic signal is well approximated by a plane wave. If this were not the case, the motion would simply induce some large, nonharmonic change in the signal that has no simple spectral interpretation. Note that the plane-wave-like approximation need be valid only along the one-dimensional curves defined by the motion, not in the full three-dimensional region surrounding them. For example, as in oceanographic applications, the medium may have strong vertical variations in the sound speed on scales smaller than the wavelength, but be nearly translation invariant in the horizontal. The vertical variation of the acoustic signal may then be quite complicated (e.g., described by a vertically localized waveguide mode profile), but the horizontal variation will be plane-wave like. Only horizontal source or receiver motion will then produce a well defined Doppler shift.

(3) Since the wavelength λ decreases with increasing frequency, the criterion (1.2) depends strongly on the source frequency ω_0. The lower the frequency, the greater the restrictions on allowed motion. In the ocean the sound speed is of order 1500 m/s, and typical vertical variations in the sound speed occur on a scale $\xi_V \simeq 100$ m. The condition $\lambda/\xi_V < 0.1$, say, restricts motion to horizontal for frequencies below about 150 Hz. If there is significant horizontal variation in the medium on some scale $\xi_H \gg \xi_V$, there will be a corresponding lower bound on the allowed frequency even for horizontal motion, given by ξ_V/ξ_H times the vertically limited frequency.

(4) Given the previous restriction on source and receiver trajectories, condition (1.3) on the acceleration remains unchanged: the velocities should not change substantially as the source or receiver travels many wavelengths.

(5) Condition (1.4) shows that the velocity scale v plays no *qualitative* role in the Doppler analysis. Higher velocities lead to larger Doppler shifts, but impose no extra conditions on the sound speed profile or on the accuracy to which the shift can be measured. Quantitative changes, as a function of the ratio v/c, will of course occur. This simple observation already hints that Doppler shifts are not a perturbative phenomenon, but must be understood in a broad context in which the actual size of v plays a lesser role.

(6) It transpires that the mathematical properties of the acoustic field that lead to well defined Doppler shift effects are very general and may be formulated independently of the more specific properties of the underlying dynamical equation. The formal results of this paper, presented in Sec. VI, should therefore find future application to larger classes of wave equations for which the required mathematical structure can be established.

The results derived in this paper should have a number of practical applications. There has been enormous progress in the past two decades in incorporating ocean environment models into analysis of low frequency, long distance sound propagation along the ocean waveguide (SOFAR channel) [5,6]. Matched field processing (MFP) methods for source localization and environmental inversion are well developed in the case of fixed sources and receivers [7,8]. However, there are important applications in which moving sources are to be passively detected in noisy and highly variable environments. A key goal is to process sonar array data to estimate the range, bearing, and speed of the source, perhaps in the presence of much louder interfering sources. MFP is a powerful approach, but requires very accurate modeling of both the ocean environment and Doppler effects. The former incorporates the strong reflection and refraction effects that exist in the ocean environment, while the present results for the latter should help mitigate motion degradation effects (Doppler broadening) and permit increased signal integration times that are crucial to extracting a low level signal from a noisy background. In addition, the results may be used in the formulation of matched field *inversion* problems, which use acoustic data to actually estimate environmental parameters using both stationary and moving receivers and sources.

The remainder of this paper is organized as follows. In Secs. II and III the basic mathematical problem is defined. In Sec. IV the high frequency, geometrical optics limit, where a ray picture of the signal propagation emerges, is considered. This allows one to examine a regime in which there exists a straightforward classical interpretation. In Sec. V, as an introduction to acoustic eigenmode ideas to be used later, it is shown how the ray picture may be formulated in terms of high frequency acoustic eigenmodes in the case of range independent media. In Sec. VI the general theory is developed under the conditions only that Eqs. (1.3) and (1.4) hold. The Doppler shift emerges from a stationary phase approximation in which the large parameter $N = \xi/\lambda$ controls the asymptotic analysis. In Sec. VII the special case of a range-independent medium, where sound speed depends only on the vertical coordinate, is considered. This case has been considered previously in Refs. [1,2], but with explicit results only for the case of a stationary receiver, and in Ref. [4] using a generalization to a nonstationary receiver that is valid only at small velocities. In Sec. VIII range-dependent media are considered in the limit of very slow horizontal variation where the commonly used adiabatic approximation is valid. This case provides an interesting example where the mathematical

requirements on the Green function are indeed obeyed by the solutions to the acoustic equation. We comment on previous formulations [3,4] of this case. The paper is concluded in Sec. IX and the key results summarized with an eye toward future numerical implementation.

II. PRELIMINARIES

The acoustic scalar wave equation is considered in either the time domain,

$$\left[\frac{1}{c^2}\partial_t^2 - \rho\,\nabla\cdot\frac{1}{\rho}\,\nabla\right]\phi(\mathbf{x},t) = S(\mathbf{x},t), \tag{2.1}$$

or frequency domain,

$$-\left[\frac{\omega^2}{c^2} + \rho\,\nabla\cdot\frac{1}{\rho}\,\nabla\right]\hat{\phi}(\mathbf{x},\omega) = \hat{S}(\mathbf{x},\omega), \tag{2.2}$$

where ϕ is the pressure field, S is the source, and $\rho(\mathbf{x})$, $c(\mathbf{x})$ are, respectively, the (position-dependent) steady state fluid density and sound speed. The Fourier transform pair is defined by

$$\hat{\phi}(\mathbf{x},\omega) = \int_{-\infty}^{\infty} dt\,\phi(\mathbf{x},t)e^{i\omega t},$$

$$\phi(\mathbf{x},t) = \int_{-\infty}^{\infty}\frac{d\omega}{2\pi}\hat{\phi}(\mathbf{x},\omega)e^{-i\omega t}, \tag{2.3}$$

and similarly for S, $\hat{S}$. Quantitative description of a number of ocean acoustic phenomena require an additional coupling to the elastic sub-bottom medium, described by a *vector* elastic wave equation with multiple polarization-dependent sound speeds. Widely used acoustic codes, such as KRAKEN [9], account explicitly for such effects. Although in this work only the scalar equation is considered, most of the formal results carry over to the vector case with trivial modifications, so long as source and receiver are located in the ocean column itself. The required generalizations will be indicated at various points in what follows.

The formal solution to Eq. (2.1) may be expressed in the form

$$\phi(\mathbf{x},t) = \int dt' \int d^3x' G(\mathbf{x},\mathbf{x}';t-t')S(\mathbf{x}',t'), \tag{2.4}$$

where the Green function G satisfies [10]

$$\left[\frac{1}{c^2}\partial_t^2 - \rho\,\nabla\cdot\frac{1}{\rho}\,\nabla\right]G(\mathbf{x},\mathbf{x}';t-t') = \delta(\mathbf{x}-\mathbf{x}')\delta(t-t'). \tag{2.5}$$

Causality implies that G vanishes for $t<t'$, so that the t' integral in Eq. (2.4) is in fact restricted to this domain.

By Fourier transforming Eq. (2.4) one obtains

$$\hat{\phi}(\mathbf{x},\omega) = \int d^3x'\hat{G}(\mathbf{x},\mathbf{x}';\omega)\hat{S}(\mathbf{x}';\omega), \tag{2.6}$$

in which $\hat{G}$ is the solution to

$$-\left(\rho\,\nabla\cdot\frac{1}{\rho}\,\nabla + \frac{\omega^2}{c^2}\right)\hat{G}(\mathbf{x},\mathbf{x}';\omega) = \delta(\mathbf{x}-\mathbf{x}'). \tag{2.7}$$

In particular, a stationary point source $S(\mathbf{x},t)=S_0(t)\,\delta(\mathbf{x}-\mathbf{x}_s)$ produces an acoustic field

$$\hat{\phi}(\mathbf{x},\omega) = \hat{G}(\mathbf{x},\mathbf{x}_s;\omega)\hat{S}_0(\omega), \tag{2.8}$$

where $\hat{S}_0(\omega)$ is the Fourier transform of $S_0(t)$.

III. MOVING SOURCES AND RECEIVERS

Consider now a moving point source $S(\mathbf{x},t)=S_0(t)\,\delta[\mathbf{x}-\mathbf{x}_s(t)]$, where $\mathbf{x}_s(t)$ is the source position and $S_0(t)$ is the signal in the reference frame of the source. We allow the receiver position $\mathbf{x}_r(t)$ to move as well. From Eq. (2.2) the measured signal is

$$\phi_0(t) \equiv \phi[\mathbf{x}_r(t),t] = \int dt' G[\mathbf{x}_r(t),\mathbf{x}_s(t');t-t']S_0(t'). \tag{3.1}$$

Viewed as a function of $\mathbf{x}_r$ at fixed t, this is the function whose wave fronts are plotted in Fig. 1 for a harmonic source. Since the two time dependencies now appear in the *spatial* arguments of G, the Fourier transform no longer has the simple factorization (2.8). This can be seen more explicitly by substituting the temporal Fourier representations of ϕ_0, S_0, and G:

$$\hat{\phi}_0(\omega) = \int\frac{d\omega'}{2\pi}\hat{S}_0(\omega')\int\frac{d\omega''}{2\pi}\int dt\,e^{i(\omega-\omega'')t} \times\int dt' e^{i(\omega''-\omega')t'}\hat{G}[\mathbf{x}_r(t),\mathbf{x}_s(t');\omega'']. \tag{3.2}$$

In the limit where $\mathbf{x}_r$, $\mathbf{x}_s$ are time independent, the two time integrals yield delta functions that enforce $\omega=\omega'=\omega''$, and Eq. (2.8) is recovered. Otherwise, the remaining integrals operate nontrivially on the spatial dependence of $\hat{G}$.

Direct numerical implementation of Eq. (3.1) is extremely time consuming [11], and is inappropriate where rapid data processing is required. The main goal of this paper is to derive forms that may be more efficiently implemented when certain uniformity conditions on the sound speed variation are satisfied.

When condition (1.3) on the acceleration holds, in the neighborhood of any given reference time t_0 one may use a local constant velocity approximation:

$$\mathbf{x}_r(t) = \mathbf{x}_r^0 + \mathbf{v}_r(t-t_0),$$

$$\mathbf{x}_s(t') = \mathbf{x}_s^0 + \mathbf{v}_s(t'-t_0), \tag{3.3}$$

where $\mathbf{x}_s^0$ and $\mathbf{x}_r^0$ are conveniently chosen reference positions. One should view $\mathbf{v}_r$ and $\mathbf{v}_s$ as being weakly dependent on t_0 on a time scale determined by Eq. (1.3). Assuming for the moment that Eq. (3.3) is valid for all times, one observes that the time integrations in Eq. (3.2) correspond to partial spatial Fourier transforms of $\hat{G}$ along the rays defined by Eq. (3.3).

In general, these correspond to separate transforms in the two spatial coordinates. However, simplification occurs in the special case where G is translation invariant in the plane defined by $\mathbf{v}_r$ and $\mathbf{v}_s$. If $\mathbf{r}$, $\mathbf{r}'$ are two-dimensional vectors in this plane, G is a function only of the difference variable $\mathbf{r}-\mathbf{r}'$, with $\mathbf{r}=\mathbf{r}_r^0+\mathbf{v}_r(t-t_0)$ and $\mathbf{r}'=\mathbf{r}_s^0+\mathbf{v}_s(t'-t_0)$ [12]. One obtains

$$\hat{\phi}_0(\omega)=\int \frac{d^2k}{(2\pi)^2}e^{i\mathbf{k}\cdot[\mathbf{r}_r^0-\mathbf{r}_s^0-(\mathbf{v}_r-\mathbf{v}_s)t_0]} \times\hat{S}_0[\omega+\mathbf{k}\cdot(\mathbf{v}_r-\mathbf{v}_s)]\tilde{G}(\mathbf{k};z_r^0,z_s^0;\omega+\mathbf{k}\cdot\mathbf{v}_r), \quad (3.4)$$

where $\tilde{G}$ is the spatial Fourier transform of $\hat{G}$ in this difference variable. In the present notation $\mathbf{r}$ and $\mathbf{r}'$ are taken to lie in the xy plane, and we decompose $\mathbf{x}_r^0=(\mathbf{r}_r^0,z_r^0)$, $\mathbf{x}_s^0=(\mathbf{r}_s^0,z_s^0)$. For a pure unit amplitude tone, $\hat{S}_0(\omega)=2\pi\delta(\omega-\omega_0)$, the inverse Fourier transform of Eq. (3.4) yields the time domain signal

$$\phi_0(t)=e^{-i\omega_0 t}\int \frac{d^2k}{(2\pi)^2}e^{i\mathbf{k}\cdot\mathbf{r}_{rs}(t)}\tilde{G}(\mathbf{k};z_r^0,z_s^0;\omega_0+\mathbf{k}\cdot\mathbf{v}_s), \quad (3.5)$$

where $\mathbf{r}_{rs}(t)=\mathbf{r}_r^0-\mathbf{r}_s^0+(\mathbf{v}_r-\mathbf{v}_s)(t-t_0)$ is the horizontal separation vector at time t.

Equations (3.4) and (3.5) (with $t_0=0$) are identical to the basic results, Eqs. (15) and (16), of Schmidt and Kuperman [4]. Notice that the Doppler shift in principle, through the wave-vector integral, couples the measured frequency ω at the receiver to the entire spectrum of source frequencies $\omega'=\omega+\mathbf{k}\cdot(\mathbf{v}_r-\mathbf{v}_s)$, with amplitude given by the Green function at yet another frequency $\omega''=\omega+\mathbf{k}\cdot\mathbf{v}_r$ (though one observes that $\omega=\omega''$ for a stationary receiver). In the limit where $\mathbf{v}_s=\mathbf{v}_r=0$, the wave number integration decouples from the frequency dependence, and one recovers Eq. (2.8) with $\mathbf{x}=\mathbf{x}_r^0$ and $\mathbf{x}_s=\mathbf{x}_s^0$.

The Fourier transform (3.2) is a *global* functional of $\phi_0(t)$, sensitive for each ω to its values at *all* times. Therefore Eq. (3.4), with its extension of the local velocity values to all time, in general differs substantially from the exact $\hat{\phi}_0(\omega)$ which necessarily incorporates the full t_0 dependence of $\mathbf{v}_r$ and $\mathbf{v}_s$. However, experimental Fourier transform data is actually collected over sequential windows with some finite width Δt [13]. The data therefore consist of the Fourier transform of the product of $\phi_0(t)$ with a window function $w(t-t_0)$:

$$\begin{aligned}\hat{\phi}_{t_0}(\omega)&\equiv\int dt w(t-t_0)\phi_0(t)e^{i\omega t}\\&=\int\frac{d\omega'}{2\pi}e^{i\omega' t_0}\hat{w}(\omega')\hat{\phi}_0(\omega-\omega')\\&=e^{i(\omega-\omega_0)t_0}\int\frac{d^2k}{(2\pi)^2}\hat{w}[\omega-\omega_0+\mathbf{k}\cdot(\mathbf{v}_r-\mathbf{v}_s)]\\&\quad\times e^{i\mathbf{k}\cdot(\mathbf{r}_r^0-\mathbf{r}_s^0)}\tilde{G}(\mathbf{k};z_r^0,z_s^0;\omega_0+\mathbf{k}\cdot\mathbf{v}_s). \quad (3.6)\end{aligned}$$

The Fourier transform $\hat{w}$ of the window function has width $2\pi/\Delta t$, limiting the range of $\mathbf{k}$ contributing to the final integral. One of the central results of this paper will be simple expressions for these window transforms.

Numerical implementation of Eq. (3.4) or (3.6) remains quite involved due to the required two-dimensional wavenumber integration. Schmidt and Kuperman [4] make a further simplification with the replacement

$$\mathbf{k}\cdot\mathbf{v}_r\to k\hat{\mathbf{n}}_{rs}\cdot\mathbf{v}_r,$$

$$\mathbf{k}\cdot\mathbf{v}_s\to k\hat{\mathbf{n}}_{rs}\cdot\mathbf{v}_s, \quad (3.7)$$

where $\hat{\mathbf{n}}_{rs}$ is the unit vector along $\mathbf{r}_{rs}(t_0)=\mathbf{r}_r^0-\mathbf{r}_s^0$. Thus the arguments of $\hat{w}_0$ and $\tilde{G}$ in Eq. (3.6) are replaced by $\omega-\omega_0+k\hat{\mathbf{n}}_{rs}\cdot(\mathbf{v}_r-\mathbf{v}_s)$ and $\omega_0+k\hat{\mathbf{n}}_{rs}\cdot\mathbf{v}_s$, respectively. These depend only on $k=|\mathbf{k}|$, and one may perform the angular integration to obtain

$$\hat{\phi}_{t_0}(\omega)\approx\int_0^\infty\frac{kdk}{2\pi}J_0(k|\mathbf{r}_r^0-\mathbf{r}_s^0|)\hat{w}[\omega-\omega_0+k\hat{\mathbf{n}}_{rs}\cdot(\mathbf{v}_r-\mathbf{v}_s)] \times\tilde{G}(k;z_r^0,z_s^0;\omega_0+k\hat{\mathbf{n}}_{rs}\cdot\mathbf{v}_s). \quad (3.8)$$

This approximation therefore reduces evaluation of $\hat{\phi}_{t_0}$ to a one dimensional Hankel transform, for which efficient numerical implementations exist, and is argued to be accurate for large separation and small velocities where the orientation of the separation vector $\mathbf{r}_{rs}(t)$ changes very little over the course of a window time Δt. These authors use a further sequence of approximations to relate Eq. (3.8) to an expansion in terms of vertical eigenmodes, which is even simpler to implement numerically. We will show in Sec. VII that this last result (with minor modifications) agrees with the low velocity limit of Hawker's [1] rigorous results (which, as it turns out, may be trivially extended to the case of a moving receiver). The latter are in turn recovered exactly from the present theory when specialized to range-independent media.

IV. DOPPLER SHIFT CORRECTIONS AT HIGH FREQUENCIES

A. Form of the Green function

We begin the formal theory of Doppler corrections by considering the high frequency limit in which the wavelength is much shorter than all scales of variation ξ of the sound speed. In this limit the WKB approximation provides a controlled perturbation theory, yielding the Green function in the asymptotic form [5],

$$\hat{G}(\mathbf{x},\mathbf{x}';\omega)\approx\sum_j\hat{\gamma}_j^{(0)}(\mathbf{x},\mathbf{x}')e^{i\omega\tau_j(\mathbf{x},\mathbf{x}')}$$

$$G(\mathbf{x},\mathbf{x}';t-t')\approx\sum_j\hat{\gamma}_j^{(0)}(\mathbf{x},\mathbf{x}')\delta[t-t'-\tau_j(\mathbf{x},\mathbf{x}')], \quad (4.1)$$

in which the sum is over all classical ray trajectories from $\mathbf{x}$ to $\mathbf{x}'$ (obeying Fermat's principle), with (minimal) travel time

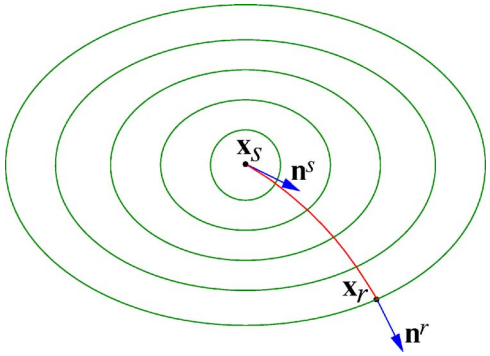

FIG. 2. (Color online) Schematic illustration of the high frequency ray theory. The fronts are surfaces of constant travel time τ from a fixed source position $\mathbf{x}_s$. A given trajectory with an initial direction $\hat{\mathbf{n}}^s$, connecting $\mathbf{x}_s$ to a given receiver position $\mathbf{x}_r$, is always normal to these fronts, and arrives at $\mathbf{x}_r$ traveling, in general, in a different direction $\hat{\mathbf{n}}^r$. In this illustration the speed of sound increases to the left and right, and decreases upwards and downwards.

$$\tau_j(\mathbf{x},\mathbf{x}') = \int_0^s \frac{ds'}{c[\mathbf{x}_j(s')]}, \tag{4.2}$$

where $\mathbf{x}_j(s')$ is the path of the jth ray, parametrized by arc length, satisfying the Eikonal equation $|\nabla\tau|^2 = 1/c^2$, with $\mathbf{x}_j(0)=\mathbf{x}'$ and $\mathbf{x}_j(s)=\mathbf{x}$ (see Fig. 2 for an illustration). For small s/ξ one finds $\tau_j(\mathbf{x},\mathbf{x}') \approx |\mathbf{x}-\mathbf{x}'|/c(\mathbf{x}')$. The amplitude is

$$\hat{\gamma}_j^{(0)}(\mathbf{x},\mathbf{x}') = \sqrt{\frac{\rho(\mathbf{x})}{\rho(\mathbf{x}')}} \lim_{s_0\to 0} \frac{1}{4\pi s_0} \times \exp\left\{-\frac{1}{2}\int_{s_0}^s ds' c[\mathbf{x}_j(s')]\nabla^2\tau[\mathbf{x}_j(s')]\right\}, \tag{4.3}$$

where the logarithmic singularity in the exponent yields $\gamma_j^{(0)}[\mathbf{x},\mathbf{x}(s)] \to 1/4\pi s$ as $s\to 0$.

The form (4.1) predicts a sharp wave front traveling at the local speed of sound. More generally, the amplitude $\hat{\gamma}_j^{(0)}(\mathbf{x},\mathbf{x}')$ is replaced by a frequency-dependent factor $\hat{\gamma}_j(\mathbf{x},\mathbf{x}';\omega)$ with an asymptotic expansion in inverse powers of the frequency:

$$\hat{G}(\mathbf{x},\mathbf{x}';\omega) = \sum_j \hat{\gamma}_j(\mathbf{x},\mathbf{x}';\omega) e^{i\omega\tau_j(\mathbf{x},\mathbf{x}')},$$

$$G(\mathbf{x},\mathbf{x}';t-t') = \sum_j \gamma_j[\mathbf{x},\mathbf{x}';t-t'-\tau_j(\mathbf{x},\mathbf{x}')], \tag{4.4}$$

where

$$\hat{\gamma}_j(\mathbf{x},\mathbf{x}';\omega) \approx \sum_{n=0}^{\infty} (i\omega)^{-n} \hat{\gamma}_j^{(n)}(\mathbf{x},\mathbf{x}'),$$

$$\gamma_j(\mathbf{x},\mathbf{x}';\tau) \approx \hat{\gamma}_j^{(0)}(\mathbf{x},\mathbf{x}')\delta(\tau) + \theta(-\tau)\sum_{n=1}^{\infty} \frac{(-\tau)^{n-1}}{(n-1)!}\hat{\gamma}_j^{(n)}(\mathbf{x},\mathbf{x}'), \tag{4.5}$$

and $\theta(s)$ is the unit step function. More rigorously, the expansion parameter is $2\pi c/\omega\xi = \lambda/\xi$, where $\xi^{-1} \sim |\nabla c|/c, |\nabla\rho|/\rho$ is the inverse scale of the variation of the environmental parameters, and the condition $\lambda/\xi \ll 1$ coincides precisely with the condition (1.4) for the existence of a well defined Doppler shift.

The WKB formalism provides explicit expressions for the $\hat{\gamma}_j^{(n)}(\mathbf{x},\mathbf{x}')$, in the form of multiple integrals along the ray path. The difference $\hat{\gamma}_j(\mathbf{x},\mathbf{x}';\omega) - \hat{\gamma}_j^{(0)}(\mathbf{x},\mathbf{x}')$ vanishes at large frequency and provides the continuous contribution to γ_j trailing the leading delta-function pulse. Equation (4.5) yields this continuous part in the form of a one-sided Taylor series immediately following the initial wave-front arrival. Since it is only asymptotic, the low frequency part of $\hat{\gamma}_j$ (or, equivalently, the shape of the pulse far behind the leading front, in general containing refracted parts of the signal traveling in considerably different directions) is not captured by this expansion, and a different nonperturbative method must be found. This will be the focus of later sections where an acoustic eigenmode expansion is used.

An example should clarify the origin of Eq. (4.1). In an infinite homogeneous space there is only one ray, namely the straight line from $\mathbf{x}'$ to $\mathbf{x}$, and $\tau_0(\mathbf{x},\mathbf{x}') = |\mathbf{x}-\mathbf{x}'|/c$. The corresponding function γ_0 takes the exact form

$$\gamma_0(\mathbf{x},\mathbf{x}';t-t'-\tau_0) = \frac{1}{4\pi c\tau_0}\delta(t-t'-\tau_0). \tag{4.6}$$

In a homogeneous half space there will be a second ray which undergoes a boundary reflection. The travel time is $\tau_1(\mathbf{x},\mathbf{x}') = |\mathbf{x}-\bar{\mathbf{x}}'|/c$, where $\bar{\mathbf{x}}' = (x',y',-z')$ is the mirror reflection of $\mathbf{x}'$ through the boundary, and γ_1 is given by the negative of Eq. (4.6) with τ_1 replacing τ_0. In a homogeneous slab of finite width h_0 there will be an infinite number of rays corresponding to multiple reflections with increasingly later arrival times $\tau_{j\pm} = |\mathbf{x}-\bar{\mathbf{x}}'_{j\pm}|/c$, where $\bar{\mathbf{x}}'_{j\pm} = (x',y',2jh_0 \pm z')$, with $j = 0, \pm 1, \pm 2, \pm 3, \ldots$, and $\gamma_{j\pm}$ given by $\pm(-1)^j$ times Eq. (4.6) with $\tau_{j\pm}$ replacing τ_0.

In this example, the zeroth order form (4.1) turns out to be exact, and the rays consist of straight line segments. Ray bending, along with the trailing part of the pulse, would be generated by variations of the sound speed within the slab. For nearly horizontal rays in a waveguide, the arrivals will correspond to rays with different numbers of oscillations within the channel. It is clear that for large j the different continuous contributions to G will start to run together, and the decomposition (4.4) becomes ambiguous for that part of the signal. In addition, we have neglected acoustic damping terms in Eq. (2.1), which act preferentially on the high frequency components of the signal and will serve to increasingly broaden even the delta-function contribution as j increases. However, in analyzing data from a high frequency source [which, via Eq. (2.8), suppresses the low frequency parts of the Green function] the decomposition (4.4) should be unambiguous. The lower frequency part of the Green function, for which the geometrical optics approximation breaks down, will be addressed in the general theory of Sec. VI.

B. Doppler theory

Equation (4.4) is now used to derive simple expressions for the Doppler shift correction. The functions τ_j and γ_j are assumed to be smooth in their explicit $\mathbf{x}$, $\mathbf{x}'$ dependence [though, as seen in Eq. (4.1), the implicit dependence through the third argument of γ_j is extremely unsmooth]. We therefore approximate

$$\gamma_j[\mathbf{x}_r(t),\mathbf{x}_s(t');t-t'-\tau_j] \approx A_j^r(t)A_j^s(t')\gamma_j(\mathbf{x}_r^0,\mathbf{x}_s^0;t-t'-\tau_j),$$

$$\tau_j[\mathbf{x}_r(t),\mathbf{x}_s(t')] \approx \tau_j^0 + \mathbf{w}_j^r\cdot\delta\mathbf{x}_r(t) - \mathbf{w}_j^s\cdot\delta\mathbf{x}_s(t') \quad (4.7)$$

in which we have defined

$$A_j^r(t) = 1 + \mathbf{K}_j^r\cdot\delta\mathbf{x}_r(t), \quad \mathbf{K}_j^r = \nabla_r \ln\,\hat{\gamma}_j^{(0)}(\mathbf{x}_r^0,\mathbf{x}_s^0),$$

$$A_j^s(t') = 1 + \mathbf{K}_j^s\cdot\delta\mathbf{x}_s(t'), \quad \mathbf{K}_j^s = \nabla_s \ln\,\hat{\gamma}_j^{(0)}(\mathbf{x}_r^0,\mathbf{x}_s^0),$$

$$\tau_j^0 = \tau_j(\mathbf{x}_r^0,\mathbf{x}_s^0), \quad (4.8)$$

and ∇_r, ∇_s are gradients with respect to the receiver and source arguments, respectively. In the case of locally linear motion in the neighborhood of a reference time t_0 one has

$$\delta\mathbf{x}_r(t) = \mathbf{v}_r(t-t_0), \quad \delta\mathbf{x}_s(t') = \mathbf{v}_s(t'-t_j'),$$

$$t_j' \equiv t_0 - \tau_j^0, \quad (4.9)$$

where, due to the time-of-flight delay, the receiver position is measured relative to its retarded time position. Note that the t_j' are *different* for each j, so that in general, for large source-receiver separation or large j, the relevant source velocity will vary with j [14]. The *slowness vectors* in the neighborhood of the source and receiver are defined by

$$\mathbf{w}_j^r = \nabla_r\tau_j(\mathbf{x}_r^0,\mathbf{x}_s^0) = \frac{1}{c(\mathbf{x}_r^0)}\hat{\mathbf{n}}_j^r,$$

$$\mathbf{w}_j^s = -\nabla_s\tau_j(\mathbf{x}_r^0,\mathbf{x}_s^0) = \frac{1}{c(\mathbf{x}_s^0)}\hat{\mathbf{n}}_j^s, \quad (4.10)$$

where $\hat{\mathbf{n}}_j^r$ and $\hat{\mathbf{n}}_j^s$ denote the ray directions at receiver and source, respectively.

The form (4.7) relies on the assumption that a single overall amplitude scale and a single time shift suffices to describe γ_j, i.e., that small shifts in $\mathbf{x}$, $\mathbf{x}'$ lead only to an overall change in the scale of the signal, and to a shift in its time origin, not to a more complicated change in its shape. This assumption certainly holds for the form (4.6), and we have argued that it will generalize to inhomogeneous media in the immediate neighborhood of the leading pulse which dominates the high frequency components of the Green function. Implicit here also is the assumption that rapid changes in the environment, for example source or receiver passing in or out of the shadow of a significant bathymetric perturbation, do not occur in the neighborhood of t_0—this is part of the condition (1.4). Such events may be expected in real data, but probably only for limited periods of time which may identified and treated separately.

By incorporating Eq. (4.7) into Eq. (3.1), the received signal takes the form

$$\phi_0(t) = \sum_j \phi_j(t),$$

$$\phi_j(t) = A_j^r(t)\int dt' A_j^s(t')S_0(t')\gamma_j\left[\mathbf{x}_r^0,\mathbf{x}_s^0;\frac{t-t_0}{\Delta_j^r} - \frac{t'-t_j'}{\Delta_j^s}\right], \quad (4.11)$$

in which the source and receiver Doppler scalings for each arrival are

$$\Delta_j^r \equiv \frac{1}{1-\mathbf{w}_j^r\cdot\mathbf{v}_r}, \quad \Delta_j^s \equiv \frac{1}{1-\mathbf{w}_j^s\cdot\mathbf{v}_s}. \quad (4.12)$$

Each term in Eq. (4.11) may separately be put in a form that mimics the signal for stationary source and receiver [over the limited time interval about t_0 in which the modified Taylor expansion (4.7) remains valid]: let us define

$$\tilde{\phi}_j(s) = \frac{1}{1+\Delta_j^r\mathbf{K}_j^r\cdot\mathbf{v}_r s}\phi_j(t_0+\Delta_j^r s),$$

$$\tilde{S}_j(s') = \Delta_j^s(1+\Delta_j^s\mathbf{K}_j^s\cdot\mathbf{v}_s s')S(t_j'+\Delta_j^s s'), \quad (4.13)$$

which incorporate independent amplitude and time rescaling for source and measured fields. Then the effective static relation

$$\tilde{\phi}_j(s) = \int ds'\tilde{S}_j(s')\gamma_j(\mathbf{x}_r^0,\mathbf{x}_s^0;s-s') \quad (4.14)$$

holds, with total measured signal

$$\phi_0(t) = \sum_j [1+\mathbf{K}_j^r\cdot\mathbf{v}_r(t-t_0)]\tilde{\phi}_j\left(\frac{t-t_0}{\Delta_j^r}\right). \quad (4.15)$$

The prefactors in Eq. (4.13) compensate for the gradual, motion-induced variation in the signal amplitude, while the time rescalings compensate for the true Doppler shift, producing the final staticlike relation (4.14) in which both effects have been removed from the data over a limited time window.

Let $\hat{S}_j(\omega)$, $\hat{\phi}_j(\omega)$, and $\hat{\gamma}_j(\mathbf{x}_r^0,\mathbf{x}_s^0;\omega)$ be the Fourier transforms of $\tilde{S}_j(s')$, $\tilde{\phi}_j(s)$, and $\gamma_j(\mathbf{x}_r^0,\mathbf{x}_s^0;s)$, respectively. In the frequency domain the results take the form

$$\hat{S}_j(\omega) = \left(1 - i\Delta_j^s\mathbf{K}_j^s\cdot\mathbf{v}_s\frac{\partial}{\partial\omega}\right)e^{-i\omega t_j'/\Delta_j^s}\hat{S}(\omega/\Delta_j^s),$$

$$\hat{\phi}_j(\omega) = \hat{\gamma}_j(\mathbf{x}_r^0,\mathbf{x}_s^0;\omega)\hat{S}_j(\omega),$$

$$\hat{\phi}_0(\omega) = e^{i\omega t_0}\sum_j \Delta_j^r\left(1 - i\mathbf{K}_j^r\cdot\mathbf{v}_r\frac{\partial}{\partial\omega}\right)\hat{\phi}_j(\Delta_j^r\omega). \quad (4.16)$$

These are once again meaningful only when convolved, via Eq. (3.6), with a window function about the reference time t_0. Great simplification occurs in the further approximation where the amplitude rescalings involving $\mathbf{K}_j^r$, $\mathbf{K}_j^s$ are dropped (expected to be valid for sufficiently small windows about t_0 and/or for sufficiently distant sources). One obtains

$$\hat{\phi}_0(\omega) = e^{i\omega t_0} \sum_j \Delta_j^r e^{-i\omega(\Delta_j^r/\Delta_j^s)t_j'} \hat{\gamma}_j(\mathbf{x}_r^0, \mathbf{x}_s^0; \Delta_j^r \omega) \hat{S}\left(\frac{\Delta_j^r}{\Delta_j^s}\omega\right), \tag{4.17}$$

which decomposes the frequency dependence of the measured signal into a sum of terms in which the source signal is Doppler shifted by both source and receiver motion, while the Green function is Doppler shifted only by the receiver motion. Note, however, that at high frequencies where these results are most valid, $\hat{\gamma}_j \to \hat{\gamma}_j^{(0)}$ becomes frequency independent. If $\hat{S}(\omega) = 2\pi\delta(\omega - \omega_0)$ represents a pure tone, $\hat{\phi}_0(\omega)$ becomes a spectrum of delta functions [and $\phi_0(t)$ a corresponding superposition of pure harmonics] at the Doppler shifted frequencies $\omega_j^D = (\Delta_j^s/\Delta_j^r)\omega_0 \approx \omega_0(1 + \mathbf{w}_j^s \cdot \mathbf{v}_s - \mathbf{w}_j^r \cdot \mathbf{v}_r)$ (where the approximate form is valid for small v/c). The appropriately windowed spectrum is therefore

$$\hat{\phi}_{t_0}(\omega) = e^{i(\omega-\omega_0)t_0} \sum_j \Delta_j^r e^{i\omega_0 \tau_j^0} \hat{w}(\omega - \omega_j^D) \hat{\gamma}_j(\mathbf{x}_r^0, \mathbf{x}_s^0; \Delta_j^s \omega_0). \tag{4.18}$$

The time delays $\tau_j^0 = \tau_j(\mathbf{x}_r^0, \mathbf{x}_s^0)$ and reference times t_0 and t_j' enter Eq. (4.17) through exponential prefactors. The large distribution of such times implies that the exponent in the *correction factor* $e^{i\omega(1-\Delta_j^r/\Delta_j^s)t_j'}$ (relative to the stationary result $e^{i\omega\tau_j^0}$) could be of order unity or larger even for very small source and receiver velocities. Thus the Doppler shift introduces significant changes in the relative phases of the terms in the sum, an effect that is clearly not accounted for by a naive Taylor expansion in $\mathbf{v}_r$ and $\mathbf{v}_s$. As a rough estimate, for frequency 100 Hz, sound speed 1500 m/s and source or receiver velocity 5 m/s, the Doppler factors will be a few times 10^{-3}, and the phase change will become significant for time delays of order 1 s, i.e., for path length differences of order 1 km, and thus readily observable in typical applications.

In many experimental realizations [5], the source signal consists of a short duration, relatively high frequency pulse. Since each γ_j represents the propagation of a single wave front through the receiver position, when convolved with the source signal according to Eq. (3.1), one expects the received signal to consist of a single short duration pulse immediately following the classical delay time τ_j^0. Through the different time delays, the different γ_j are sensitive to different parts of the source signal history for a given fixed measurement time t. In the case of a medium with multiple boundaries, or waveguide regions, the spectrum of time delays will be extremely broad: the amplitude of the full Green function G may be expected to decay as a power of $1/t$, eventually cut off by dissipative loss mechanisms. It is this very long system memory that precludes a more direct perturbation theory in the velocities $\mathbf{v}_r$ and $\mathbf{v}_s$. This is the time-domain counterpart of the frequency-domain phase factor corrections.

The previous results are rather formal. In applications, the key parameters τ_j, $\mathbf{w}_j^s$, $\mathbf{w}_j^r$, $\mathbf{K}_j^s$, $\mathbf{K}_j^r$ must be computed explicitly for the given sound speed profile. Fortunately, they all follow directly from the leading behavior (4.1), which may be determined via standard dynamic ray tracing methods [5,6]. Optimal agreement with data will, of course, occur when $\hat{S}_0(\omega)$ is confined to high frequencies where one may simply use $\hat{\gamma}_j(\mathbf{x}, \mathbf{x}'; \omega) = \hat{\gamma}_j^{(0)}(\mathbf{x}, \mathbf{x}')$ in Eq. (4.17), in which case ray methods determine all required parameters. If results are required at a somewhat lower frequency [but not so low that the Doppler condition (1.4) breaks down], rather than computing higher terms in the expansion (4.5) via (extremely cumbersome) ray techniques, one often has available an efficient method for computing the Green function itself (e.g., via an acoustic eigenmodal decomposition) at a sequence of frequencies ω_l. Assuming that the frequency dependence of $\hat{\gamma}_j(\mathbf{x}, \mathbf{x}'; \omega)$ is fairly weak, one might use the ray results for the delay times τ_j and then *fit* the $\hat{\gamma}_j$ via solution of the set of suitably truncated linear equations

$$\hat{G}(\omega_l) = \sum_{j=1}^{j_{\max}} \hat{\gamma}_j(\bar{\omega}) e^{i\omega_l \tau_j}, \quad l = 1, 2, \ldots, l_{\max}, \tag{4.19}$$

in which it is assumed that the chosen frequencies are sufficiently closely spaced about some value $\bar{\omega}$ that $\hat{\gamma}_j(\omega_l) = \hat{\gamma}_j(\bar{\omega})$ is essentially constant, while the phase factors $e^{i\omega_l\tau_j}$ vary substantially. This procedure may be repeated for different values of $\bar{\omega}$ covering the domain of $\hat{S}_0(\omega)$.

An alternative, but related, approach is to focus on the wave-number spectrum in the neighborhood of the receiver. Thus we write

$$G(\mathbf{x}_0 + \delta\mathbf{x}, \mathbf{x}'; t - t') \approx \mathrm{Re} \int \frac{d^3k}{(2\pi)^3} e^{ik[\hat{\mathbf{n}} \cdot \delta\mathbf{x} - c(\mathbf{x}_r)(t-t')]} \times \hat{g}(k, \hat{\mathbf{n}}; \mathbf{x}_r, \mathbf{x}'),$$

$$\hat{G}(\mathbf{x}_0 + \delta\mathbf{x}, \mathbf{x}'; \omega) \approx \int \frac{d^2\hat{\mathbf{n}}}{(2\pi)^2} e^{i\omega\hat{\mathbf{n}} \cdot \delta\mathbf{x}/c(\mathbf{x}_r)} \times [\hat{g}(\omega/c(\mathbf{x}_r), \hat{\mathbf{n}}; \mathbf{x}_r, \mathbf{x}')\theta(\omega) + \hat{g}^*(-\omega/c(\mathbf{x}_r), \hat{\mathbf{n}}; \mathbf{x}_r, \mathbf{x}')\theta(-\omega)], \tag{4.20}$$

in which $\mathbf{x}_r$ is the receiver position, $\hat{\mathbf{n}} = \mathbf{k}/k$ is the wave direction, and $\delta\mathbf{x}$ is assumed small so that we may approximate $\mathbf{c}(\mathbf{x}_0 + \delta\mathbf{x}) \simeq \mathbf{c}(\mathbf{x}_0)$. The existence of this decomposition is guaranteed at high frequency by the condition $\lambda/\xi \ll 1$, where ξ is in this case the scale of variation of the sound speed in the neighborhood of the receiver. For a single delta-function plane wave front propagating in direction $\hat{\mathbf{n}}_0$ with amplitude $\hat{\gamma}_0$ and arriving at time τ_0, we have $\hat{g}(k, \hat{\mathbf{n}}; \mathbf{x}_0, \mathbf{x}') = \hat{\gamma}_0 k^{-2} \delta(\hat{\mathbf{n}} - \hat{\mathbf{n}}_0^r) e^{ik\mathbf{c}(\mathbf{x}_0)\tau_0}$. For a sequence of such arrivals, $\hat{g}$ will be a sum of such terms for different $\hat{\mathbf{n}}_j^r$, $\hat{\gamma}_j$, τ_j. We identify these parameters with those appearing in Eqs. (4.7)–(4.10). Given an efficient method for computing the Green function itself, Eq. (4.20) provides an alternative method for computing these parameters through its partial wave-number decomposition. The similarity between Eqs. (4.19) and (4.20) is clear since the latter now reduces to a sum over a discrete number of plane waves. Rather than using a sequence of closely spaced frequencies to invert for the amplitudes $\hat{\gamma}_j(\bar{\omega})$, one now requires a discrete set of positions $\delta\mathbf{x}$ in order to invert for the spatial Fourier transform. Numerical tests will be required to see which method, or perhaps a hybrid of the two, is most practical.

V. RELATION BETWEEN RAY THEORY AND MODE REPRESENTATION

A very common approximation used in the description of ocean environments is a sound speed depending only on the vertical coordinate z. We summarize in this section the mode formalism needed to deal with this case, and also show how ray theory is recovered from it at high frequencies. The general results will also be used in later sections to compute Doppler shift corrections at low frequencies where ray theory is invalid.

The Green function appearing in Eq. (3.4) in this range-independent case may be expressed in the form

$$\hat{G}(\mathbf{k};z,z';\omega)=\frac{1}{\rho(z')}\sum_j \frac{\psi_j^*(z';\omega)\psi_j(z;\omega)}{k^2-k_j(\omega)^2-i\eta}, \tag{5.1}$$

where $\eta\to 0^+$ is a positive infinitesimal reflecting outgoing wave boundary conditions at infinity. The horizontal inverse Fourier transform is given by

$$\hat{G}(\mathbf{r}-\mathbf{r}';z,z';\omega)=\frac{i}{4\rho(z')}\sum_j \psi_j^*(z';\omega)\psi_j(z;\omega) \times H_0^{(1)}[k_j(\omega)|\mathbf{r}-\mathbf{r}'|], \tag{5.2}$$

where $H_0^{(1)}$ is a Hankel function. Here k_j, ψ_j are normalized solutions to eigenvalue equation

$$\left[\rho(z)\partial_z\frac{1}{\rho(z)}\partial_z+\frac{\omega^2}{c(z)^2}\right]\psi_j(z;\omega)=k_j(\omega)^2\psi_j(z;\omega),$$

$$\int \frac{dz}{\rho(z)}\psi_i^*(z;\omega)\psi_j(z;\omega)=\delta_{ij}. \tag{5.3}$$

When $k_j^2\equiv-\kappa_j^2<0$, one uses the relation $H_0^{(1)}(i\rho)=(2/i\pi)K_0(\rho)$, where K_0 is a modified Bessel function. In the far field one may use the asymptotic forms $H_0^{(1)}(\rho)\approx\sqrt{2/\pi i\rho}e^{i\rho}$, $K_0(\rho)\approx\sqrt{\pi/2\rho}e^{-\rho}$, $\rho\gg 1$. Each propagating mode (defined by $k_j^2>0$) has a well defined phase velocity $c_j^\phi=\omega/k_j$ and group velocity $c_j^g=(dk_j/d\omega)^{-1}$. The mode expansion remains valid even when there is coupling to more complicated elastic media. The only changes in that case are the boundary conditions satisfied by the ψ_j at any interfaces and their orthogonality relations.

For the uniform slab (rectangular waveguide) with Dirichlet boundary conditions and thickness h_0 one obtains

$$\psi_j(z;\omega)=\sqrt{\frac{2}{h_0}}\sin(q_jz),\ q_j\equiv j\pi/h_0,$$

$$k_j(\omega)=\sqrt{\frac{\omega^2}{c^2}-q_j^2}, \tag{5.4}$$

for $j=1,2,3,\ldots$. In this example the mode profiles are frequency independent, and the mode group and phase velocities are related via $c_j^g=c^2/c_j^\phi$, with both approaching c at high frequency for any fixed mode number j. As noted at the beginning of Sec. III, different classical ray arrivals correspond to different numbers of reflections from the two boundaries. One may define an effective horizontal group velocity $c^g(\theta)=c\cos(\theta)$ for a ray propagating at angle θ away from the horizontal. In the mode picture, for any given frequency one may define an effective propagation angle via $\tan(\theta_j)=q_j/k_j$, the ratio of vertical to horizontal wave number. Using Eq. (5.4) one obtains $c\cos(\theta_j)=ck_j/\sqrt{k_j^2+q_j^2}=c_j^g$, so that there is in this case an exact correspondence between classical ray theory and mode theory even at low frequencies. This should not be too surprising since deviations from ray theory [in the sense of broadening of the delta-function pulses (4.1)] occur only when the sound speed is inhomogeneous.

More generally, at high frequencies, where the wavelength is much smaller that the inhomogeneity length scale of $c(z)$, the mode eigenfunctions themselves have a WKB expansion [5,6]

$$\psi_j^*(z';\omega)\psi_j(z;\omega)\approx\frac{1}{\mathcal{N}_j}e^{i\int_{z'}^z dz''\sqrt{\omega^2/c(z'')^2-k_j(\omega)^2}} \times\frac{\sqrt{\rho(z')\rho(z)}}{\left[\frac{\omega^2}{c(z')^2}-k_j(\omega)^2\right]^{1/4}\left[\frac{\omega^2}{c(z)^2}-k_j(\omega)^2\right]^{1/4}}, \tag{5.5}$$

where $\mathcal{N}_j$ is a normalization. When combined with the phase factor $e^{ik_j(\omega)|\mathbf{r}-\mathbf{r}'|}$ arising from the Hankel function, the stationary phase approximation may be used to identify the terms that make the primary contribution to the sum (5.2): at high frequency $k_j(\omega)=\omega/c_j^\phi(\omega)$ becomes continuous function of j, and the stationary phase condition yields

$$|\mathbf{r}-\mathbf{r}'|=\int_{z'}^z dz''\left(\frac{c_j^\phi(\omega)^2}{c(z'')^2}-1\right)^{-1/2}. \tag{5.6}$$

It is easy to verify [5,6] that for given *fixed* $c_j^\phi(\omega)$, Eq. (5.6) produces a classical ray trajectory, classified most easily by the upper and lower turning points $\tilde{z}_\pm$ at which $c(\tilde{z}_\pm)=c_j^\phi(\omega)$. The associated group velocity $c_j^g(\omega)$ is also fixed, and is precisely the mean horizontal speed of the ray. It is seen therefore that those modes j with group velocity close to some given value determine precisely the classical ray with that same group velocity. This identification allows one to use mode theory to compute group velocities, and hence ray travel times. Moreover, the Green function (5.2) is already essentially in the plane wave form (4.20): for fixed source and receiver positions, the index j plays the role of the ray arrival direction, and should be scanned to find the largest contributing terms. These will correspond to the discrete set of ray arrivals, and provide the required ray parameters in Eqs. (4.7)–(4.10).

VI. GENERAL THEORY

In this section we consider the most general case where the assumptions that underlie the ray formulation of Sec. III are weakened, while at the same time restrictions are placed on the source and receiver trajectories. The starting point is

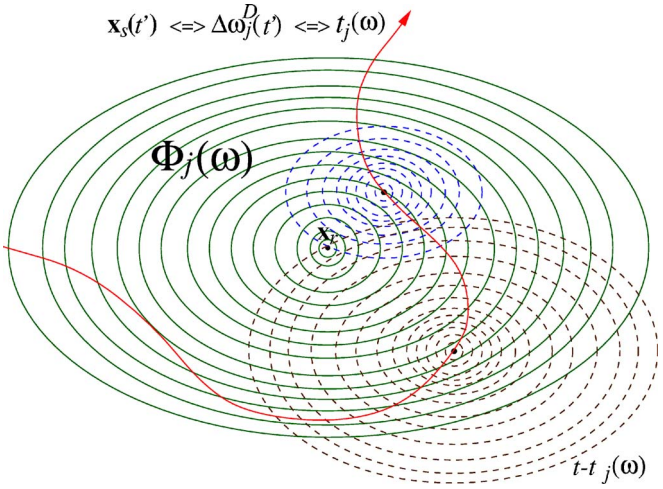

FIG. 3. (Color online) Schematic diagram illustrating the essential content of the general Doppler shift theory. The receiver position $\mathbf{x}_r$ is, for the moment, considered to be fixed, and the main set of wave fronts centered on $\mathbf{x}_r$ are the level surfaces of the phase function $\Phi_j(\mathbf{x}_r,\mathbf{x}_s;\omega)$ for some selected value of j, considered as a function of $\mathbf{x}_s$ for fixed $\mathbf{x}_r$ and ω. The actual source is shown traversing some trajectory $\mathbf{x}_s(t')$. The (fictitious) acoustic patterns, arriving at $\mathbf{x}_r$ from a *fixed* source at two different points along this trajectory, are shown simply to illustrate the time delay between t' the observation time t. There will be a special time $t'=t_j(\omega)$ (or, depending on the trajectory, perhaps a discrete set of such times) at which the received signal actually has frequency ω. The source contribution $\Delta\omega_j^s$ to the Doppler shift $\Delta\omega_j^D=\omega-\omega_0=\Delta\omega_j^s+\Delta\omega_j^r$ is determined, self-consistently, by the rate at which $\mathbf{x}_s$ was crossing the local wave fronts of Φ_j at that time—this is the content of the first stationarity condition (6.6) or (6.21). The time t at which the source shift $\Delta\omega_j^s$ is actually seen by the receiver is determined by the time of flight from $\mathbf{x}_s(t')$ to $\mathbf{x}_r$—this is the content of the second stationarity condition (6.10) or (6.22). The receiver contribution $\Delta\omega_j^r$ to the Doppler shift is finally determined by restoring the time dependence to $\mathbf{x}_r(t)$ and adding in the rate at which the receiver crosses the wave fronts of Φ_j, now viewed as a function of $\mathbf{x}_r$ for fixed $\mathbf{x}_s$ and ω. This is the content of Eq. (6.17), or of Eqs. (6.20) and (6.24).

the general formula (3.1) for the time-domain signal:

$$\phi(\mathbf{x}_r,t)=\int dt'\,G[\mathbf{x}_r,\mathbf{x}_s(t');t-t']e^{-i\omega_0 t'}$$

$$=e^{-i\omega_0 t}\int\frac{d\omega}{2\pi}e^{-i(\omega-\omega_0)t}\hat{\varphi}(\mathbf{x}_r;\omega),\qquad(6.1)$$

where

$$\hat{\varphi}(\mathbf{x}_r;\omega)\equiv\int dt'\,\hat{G}[\mathbf{x}_r,\mathbf{x}_s(t');\omega]e^{i(\omega-\omega_0)t'},\qquad(6.2)$$

in which $\mathbf{x}_r$ may in fact be time dependent as well, but for clarity we temporarily suppress this from the notation.

The derivations to follow will involve a large number of implicit relationships between quantities in the frequency and time domains, and at different retarded times. Figure 3 is intended to illustrate these, and will be referred to as that derivation proceeds.

A. Structure of the Green function

We now propose a general mathematical structure for $\hat{G}$ that will lead to well-defined Doppler shift effects. The structure, at this stage, should be considered entirely separate from the physics of the underlying acoustic equation (2.1) that defines $\hat{G}$, implying that the formal results derived in this section apply much more generally. In later sections the acoustic equation will be used to determine the physical conditions under which $\hat{G}$ possesses the required form. It would be interesting to explore other equations which lead to this structure, but this lies beyond the scope of the present work.

The general results are based on the assumption (to be verified for any given application) that the Green function may be decomposed in the form

$$\hat{G}(\mathbf{x}_r,\mathbf{x}_s;\omega)=\sum_j A_j(\mathbf{x}_r,\mathbf{x}_s;\omega)e^{i\Phi_j(\mathbf{x}_r,\mathbf{x}_s;\omega)},\qquad(6.3)$$

where, associated with each term in the sum and each point in space, there are local receiver and source wave vectors,

$$\mathbf{k}_j^r(\mathbf{x}_r,\mathbf{x}_s;\omega)=\nabla_r\Phi_j(\mathbf{x}_r,\mathbf{x}_s;\omega),$$

$$\mathbf{k}_j^s(\mathbf{x}_r,\mathbf{x}_s;\omega)=\nabla_s\Phi_j(\mathbf{x}_r,\mathbf{x}_s;\omega).\qquad(6.4)$$

Here $\mathbf{k}_j^r$ and $\mathbf{k}_j^s$, as well as the amplitude A_j are assumed to be *slowly varying,* on the scale of the local wavelengths $2\pi/|\mathbf{k}_j^r|$ and $2\pi/|\mathbf{k}_j^s|$, *at least in the direction of source (and later, receiver) motion*. Figure 3 illustrates the level surfaces of Φ_j, and the assumption is that these surfaces are locally equally spaced. Thus, if the wavelength scale is denoted by λ, and the scale of variation is denoted by ξ, then we assume that $N\equiv\xi/\lambda\gg 1$. Ray theory emerges as a special case where N is large for variations in *all* directions, not just along the source or receiver trajectories. The sum accounts for the multiple waves through any given point. The slow variation assumption implies that the dependence of the integrand of Eq. (6.2) on $\mathbf{x}_s(t')$ is, locally in time, a superposition of sinusoids with frequencies $\Delta\omega_j(t')=-\mathbf{k}_j^s\cdot\mathbf{v}_s$, where $\mathbf{v}_s=\dot{\mathbf{x}}_s$ is the instantaneous velocity, also assumed to be slowly varying over the time during which the source travels a distance of order ξ. The minus sign implies that the Doppler shift is positive when velocity and wave number are opposite.

Equation (6.3) is a very general assumption about the structure of the Green function within the acoustic medium. It in no way precludes couplings, e.g., through the ocean floor, to other elastic media described by more complicated dynamical equations. Everything that follows is based only on this assumption, and the results that follow will carry over without change to the more general physical situations.

B. Stationary phase evaluation

Intuitively, given the sinusoidal dependence of Eq. (6.2) on t', for a given frequency ω the integral should be dominated by those times t' for which $\omega-\omega_0=\Delta\omega_j(t')$: as illus-

trated in Fig. 3, the rate at which the source is crossing the wave fronts of Φ_j should match the observed Doppler shift. This idea may be stated precisely within the stationary phase approximation [15]. The integral summands may be written in the form

$$\hat{\varphi}_j(\mathbf{x}_r;\omega) \equiv \int dt' A_j[\mathbf{x}_r,\mathbf{x}_s(t');\omega] e^{i\Phi_j[\mathbf{x}_r,\mathbf{x}_s(t');\omega]} e^{i(\omega-\omega_0)t'}$$
$$= \frac{\xi}{v}\int d\tau' A_j[\mathbf{x}_r,\mathbf{x}_s(\xi\tau'/v);\omega_0+v\zeta/\lambda] \times e^{iN\{f_j[\mathbf{x}_r,\mathbf{x}_s(\xi\tau'/v);\omega_0+v\zeta/\lambda]+\zeta\tau'\}}, \quad (6.5)$$

where $f_j=\Phi_j/N$, $\zeta=\lambda(\omega-\omega_0)/v$, $\tau'=vt'/\xi$, and v is the source velocity scale. Here τ' has been defined in such a way that the source moves a distance of order ξ for order unity variation in τ', and we have observed that $\partial_{\tau'}\Phi_j=\xi\omega_j/v \sim \xi/\lambda=N$, thus motivating the definition of f_j. Since N is large, the integral is dominated by the stationary phase point $\tau'=\tau_j(\zeta)$ determined by

$$\zeta=(\lambda/v)\Delta\omega_j(\xi\tau_j/v),$$
$$\Delta\omega_j(\xi\tau_j/v) \equiv -\mathbf{k}_j^s[\mathbf{x}_r,\mathbf{x}_s(\xi\tau_j/v);\omega_0+v\zeta/\lambda]\cdot\mathbf{v}_s(\xi\tau_j/v), \quad (6.6)$$

which is identical to the condition $\omega-\omega_0=\Delta\omega_j(t')$ intuited above. The second derivative of the phase takes the form

$$f_j^{(2)}(\tau') \equiv \partial_{\tau'}^2 f_j = \frac{\lambda\xi}{v^2}[\mathbf{a}_s\cdot\mathbf{k}_j^s+(\mathbf{v}_s\cdot\nabla_s)(\mathbf{k}_j^s\cdot\mathbf{v}_s)], \quad (6.7)$$

where $\mathbf{a}_s=\partial_{t'}\mathbf{v}_s$ is the instantaneous source acceleration. The final stationary phase evaluation of $\hat{\varphi}_j$ therefore takes the form

$$\hat{\varphi}_j(\mathbf{x}_r;\omega) \approx \frac{\xi}{v}A_j[\tau_j(\zeta)]\sqrt{\frac{2\pi}{iNf_j^{(2)}[\tau_j(\zeta)]}}e^{iN[f_j[\tau_j(\zeta)]+\zeta\tau_j(\zeta)]}. \quad (6.8)$$

Substituting this form back into the first line of Eq. (6.1), one obtains

$$\phi(\mathbf{x}_r,t) = e^{-i\omega_0 t}\sum_j \varphi_j(\mathbf{x}_r,t),$$
$$\varphi_j(\mathbf{x}_r;t) \equiv \int \frac{d\omega}{2\pi}e^{-i(\omega-\omega_0)t}\hat{\varphi}_j(\mathbf{x}_r;\omega)$$
$$\approx \int \frac{d\zeta}{2\pi}A_j[\tau_j(\zeta)]\sqrt{\frac{2\pi iN}{f_j^{(2)}[\tau_j(\zeta)]}}e^{iN\tilde{f}_j(\zeta)},$$
$$\tilde{f}_j \equiv f_j[\tau_j(\zeta)]+\zeta[\tau_j(\zeta)-\tau], \quad (6.9)$$

where $\tau=vt/\xi$. Although suppressed from the notation, in addition to the explicit ζ dependence entering through $\tau_s(\zeta)$, there is further dependence via the argument $\omega=\omega_0+v\zeta/\lambda$. A stationary phase evaluation of Eq. (6.9) is again appropriate, with stationary point $\zeta=\zeta_j(\tau)$ defined by

$$(v/\lambda)\partial_\omega f_j = \tau-\tau_j(\zeta_j), \quad (6.10)$$

where the derivative is with respect to this latter dependence only. Whereas Eq. (6.6) determined only the source time τ' at which the frequency shift ζ originated, Eq. (6.10) determines the receiver time τ at which that shift will actually be observed by incorporating the time of flight—see Fig. 3. Using the stationarity condition (6.6), the second derivative of the phase now takes the form

$$\tilde{f}_j^{(2)}(\zeta) = (v/\lambda)^2\partial_\omega^2 f_j - f_j^{(2)}(\tau_j)(\partial_\zeta\tau_j)^2 = (v/\lambda)^2\partial_\omega^2 f_j - \frac{(1+f_j^{(1)})^2}{f_j^{(2)}(\tau_j)} \quad (6.11)$$

in which the ζ derivative of the stationarity condition (6.6) has been used to obtain

$$\partial_\zeta\tau_j = -\frac{1+f_j^{(1)}(\tau_j)}{f_j^{(2)}(\tau_j)}, \quad (6.12)$$

where we have defined

$$f_j^{(1)}(\tau_j) \equiv (v/\lambda)(\partial_\omega\partial_{\tau'}f_j)_{\tau'=\tau_j(\zeta_j)} = -\mathbf{v}_s\cdot\partial_\omega\mathbf{k}_j^s. \quad (6.13)$$

The final result for the received signal is

$$\varphi_j(\mathbf{x}_r;t) \approx \frac{iA_j[\tau_j(\zeta_j)]}{\sqrt{\tilde{f}_j^{(2)}(\zeta_j)f_j^{(2)}[\tau_j(\zeta_j)]}}e^{iN\tilde{f}_j(\zeta_j)}. \quad (6.14)$$

This equation is the basic result of this section. The key observation is that the time derivative of the phase yields the instantaneous Doppler shift in the frequency [since the fundamental frequency has already been removed as a prefactor in the first line of Eq. (6.9)] in the form

$$\Delta\omega_j^D(t) = -\mathbf{k}_j^r[\mathbf{x}_r(t),\mathbf{x}_s[t_j(t)];\omega_0+v\zeta_j(t)/\lambda]\cdot\mathbf{v}_r(t) - \mathbf{k}_j^s[\mathbf{x}_r(t),\mathbf{x}_s[t_j(t)];\omega_0+v\zeta_j(t)/\lambda]\cdot\mathbf{v}_s[t_j(t)], \quad (6.15)$$

in which $t_j(t)=(\xi/v)\tau_j[\zeta_j(t)]$ is the source time specified by the stationarity conditions. All other terms vanish due to the stationarity condition (6.10). It is clear, by comparing Eq. (6.15) with Eqs. (4.11) and (4.12), that in the high frequency ray limit one obtains the slowness vectors from the wave vectors via $\mathbf{k}_j^r/\omega\to\mathbf{w}_j^r$ and $\mathbf{k}_j^s/\omega\to\mathbf{w}_j^s$.

C. Signal character in a narrow time window

Consider now the nature of the signal in a neighborhood of width Δt about a reference time t_0. Here Δt should be such that the fractional change in amplitude and in the Doppler shift itself is small: for constant velocity motion in a range-independent environment the fractional change in the source-receiver separation vector should be small. On larger time scales, smearing of the Doppler shift will occur. On the other hand, meaningful measurement of the Doppler shift requires that $\Delta t \gg \tau_D \equiv 2\pi/\Delta\omega_D$, where $\Delta\omega_D\sim\omega_0 v/c$ is the scale of the Doppler shift. This is guaranteed by large N: $(v\Delta t)\times(\omega_0/2\pi c)=v\Delta t/\lambda$ is the number of uniformly spaced wave fronts traversed during the course of the measurement, and

the slow variation assumption ensures that this can be made large by choosing $\Delta t = O(\xi/v)$.

Now, the only rapidly varying part of the signal comes from the phase factor:

$$N\tilde{f}_j(\zeta_j(t),t) = N\tilde{f}_j(\zeta_j(t_0),t_0) + \Delta\omega_j^D(t_0)(t-t_0) + O[(t-t_0)^2], \tag{6.16}$$

and ignoring time variations in the amplitude factor [one could include linear variation in the amplitudes, as in Eqs. (4.7)–(4.16), but for simplicity we shall forego such complications here], one obtains in the neighborhood of t_0:

$$\phi_0(t;\omega_0) \approx e^{-i\omega_0 t_0}\sum_j B_j(t_0)e^{-i\omega_j^D(t_0)(t-t_0)},$$

$$\omega_j^D(t_0) \equiv \omega_0 + \Delta\omega_j^D(t_0),$$

$$B_j(t_0) \equiv \frac{iA_j\{\tau_j[\zeta_j(t_0)]\}}{\sqrt{\tilde{f}_j^{(2)}\{\zeta_j(t_0)\}f_j^{(2)}\{\tau_j[\zeta_j(t_0)]\}}}\, e^{iN\tilde{f}_j[\zeta_j(t_0)]}, \tag{6.17}$$

where we have explicitly included ω_0 in the notation for ϕ_0 in order to emphasize that the result is for a monochromatic source. The definition of Δt guarantees that the nonlinear correction terms in Eq. (6.16) may indeed by neglected. The *local* Fourier transform, over the time interval of width Δt centered on t_0, is now trivial to compute from Eq. (6.17):

$$\hat{\phi}_0(\omega;\omega_0) \equiv \int_{t_0-\Delta t/2}^{t_0+\Delta t/2} dt\ \phi_0(t;\omega_0)e^{i\omega t} \approx e^{-i\omega_0 t_0}\sum_j B_j(t_0)\frac{\sin[(\omega-\omega_j^D)\Delta t/2]}{(\omega-\omega_j^D)/2}. \tag{6.18}$$

This represents a special case of Eq. (3.6) in which the window function $w(t)$ is a simple indicator function on the interval $[-\Delta t/2, \Delta t/2]$. Clearly, any other window function could be used as well [as in Eq. (4.18)], replacing the sine factor in the second line of Eq. (6.17) by the window transform $\hat{w}(\omega - \omega_j^D)$.

For a general source spectrum one must compute ϕ_0 and $\hat{\phi}_0$ for the appropriate range of frequencies and form the superpositions

$$\phi_0(t) = \int \frac{d\omega_0}{2\pi}\hat{S}(\omega_0)\phi_0(t;\omega_0),$$

$$\hat{\phi}_0(\omega) = \int \frac{d\omega_0}{2\pi}\hat{S}(\omega_0)\hat{\phi}_0(\omega;\omega_0). \tag{6.19}$$

D. Summary of results in unscaled variables

The sequence of implicit relations that define the stationary phase results is quite involved, and though the scaled variables ζ and τ are most appropriate for rigorous organization of the computation, they do not provide a particularly transparent set of variables for practical implementation. We summarize here therefore the key results using the original physical frequency and time variables.

First, from Eqs. (6.4) and (6.15), the receiver and source contributions to the Doppler shifts are defined by

$$\Delta\omega_j^r[\mathbf{x}_r(t),\mathbf{x}_s(t');\omega] \equiv -\partial_t\Phi_j[\mathbf{x}_r(t),\mathbf{x}_s(t');\omega] = -\mathbf{v}_r(t)\cdot\mathbf{k}_j^r[\mathbf{x}_r(t),\mathbf{x}_s(t');\omega],$$

$$\Delta\omega_j^s[\mathbf{x}_r(t),\mathbf{x}_s(t');\omega] \equiv -\partial_{t'}\Phi_j[\mathbf{x}_r(t),\mathbf{x}_s(t');\omega] = -\mathbf{v}_s(t')\cdot\mathbf{k}_j^s[\mathbf{x}_r(t),\mathbf{x}_s(t');\omega]. \tag{6.20}$$

The theory begins by providing a mapping between the observed receiver frequency ω and the time $t'=t_j(\omega)$ at which the signal producing that (Doppler shifted) frequency left the source. This mapping is first developed for a fixed receiver position $\mathbf{x}_r$ (for which case ω is an intermediate frequency containing only the Doppler shift due to the source), and is obtained from Eq. (6.20) by solving the first stationarity condition (6.6). In physical variables the latter takes the form

$$\omega - \omega_0 = \Delta\omega_j^s[\mathbf{x}_r,\mathbf{x}_s(t_j);\omega]. \tag{6.21}$$

The intuitive content of this equation is clear: the Doppler shift associated with source motion is given by the rate at which the source is crossing the acoustic wave fronts generated by Φ_j. What is perhaps not so obvious is that the frequency at which these wave fronts are being generated is not the source frequency ω_0, but the self-consistently determined Doppler shifted frequency itself.

The theory next relates receiver and source time (also referred to as "contemporary" and "retarded" time, respectively [2]) by determining the time t at which the signal with specified frequency ω arrives at the receiver. This is the content of the second stationarity condition (6.10), which in physical variables takes the form

$$t - t_j = \frac{\partial}{\partial\omega}\Phi[\mathbf{x}_r(t),\mathbf{x}_s(t_j);\omega], \tag{6.22}$$

and is to be solved for $\omega=\omega_j(t)$. The derivative is with respect to the explicit ω dependence alone, not that implicitly contained in $t_j(\omega)$. This equation also has a nice interpretation: the left hand side is the time of flight, while the right hand side may be rewritten in the form

$$t - t_j = \int_{\mathbf{x}_s(t_j)}^{\mathbf{x}_r(t)} \frac{|d\mathbf{x}|}{v_j^g(\mathbf{x};\omega)}, \tag{6.23}$$

where $v_j^g = (\partial k_j/\partial\omega)^{-1}$ defines the magnitude of the local mode group velocity, and the integration path connecting $\mathbf{x}_s$ to $\mathbf{x}_r$ has been chosen to be everywhere normal to the surfaces of constant Φ for fixed source position, i.e., parallel to $\mathbf{k}_j[\mathbf{x},\mathbf{x}_s(t_j);\omega]$. This constitutes a version of Fermat's principle. The result (6.23) relies on the added assumption that *the path so defined lies completely within the slowly varying manifold.* This need not be the case: the manifolds around $\mathbf{x}_r$ and $\mathbf{x}_s$ could, for example, be disconnected—further com-

ments on this will given in Sec. IX—in which case (6.23) does not make sense, though Eq. (6.22) remains valid. We shall see below that Eq. (6.23) does have meaning in situations where the acoustic adiabatic approximation is valid.

The composition $t_j(t) \equiv t_j[\omega_j(t)]$ is the time at which the signal left the source in order to arrive at the receiver at time t. The total Doppler shifted frequency, including both source and receiver motion is now given by Eq. (6.15), which in terms of physical variables reads

$$\begin{aligned}\omega_j^D(t) &= \omega_j(t) + \Delta\omega_j^r\{\mathbf{x}_r(t), \mathbf{x}_s[t_j(t)]; \omega_j(t)\} \\ &= \omega_0 + \Delta\omega_j^s\{\mathbf{x}_r(t), \mathbf{x}_s[t_j(t)]; \omega_j(t)\} \\ &\quad + \Delta\omega_j^r\{\mathbf{x}_r(t), \mathbf{x}_s[t_j(t)]; \omega_j(t)\}, \end{aligned} \tag{6.24}$$

where the second term now adds in the rate at which the receiver crosses the acoustic wave fronts. Since the receiver is "passive," its motion does not affect the frequency $\omega_j(t)$ at which the wave fronts are being generated. The total signal, including amplitude factors, is now given by

$$\begin{aligned}\phi_0(t;\omega_0) &= e^{-i\omega_0 t}\mathcal{G}(t;\omega_0) \equiv e^{-i\omega_0 t}\sum_j g_j(t;\omega_0), \\ g_j(t;\omega_0) &\equiv \frac{A_j(t)}{\mathcal{N}_j(t)} e^{i\{\Phi_j(t) - [\omega_j(t) - \omega_0][t - t_j(t)]\}}, \\ A_j(t) &\equiv A_j\{\mathbf{x}_r(t), \mathbf{x}_s[t_j(t)]; \omega_j(t)\}, \\ \Phi_j(t) &\equiv \Phi_j\{\mathbf{x}_r(t), \mathbf{x}_s[t_j(t)]; \omega_j(t)\} \end{aligned} \tag{6.25}$$

in which the (square of the) normalization is given by

$$\begin{aligned}\mathcal{N}_j(t)^2 &= \left\{ [1 + \Phi_j^{(1)}(t)]^2 - \Phi_j^{(2)}(t)\frac{\partial^2\Phi_j}{\partial\omega^2} \right\}_{\omega=\omega_j(t)}, \\ \Phi_j^{(1)}(t) &\equiv \left(\frac{\partial^2\Phi_j}{\partial\omega\,\partial t'}\right)_{t'=t_j(t)} \\ &= -\left[1 + \frac{dt_j}{d\omega}\Phi_j^{(2)}(t)\right] = -[\mathbf{v}_s \cdot \partial_\omega \mathbf{k}_j^s]_{t'=t_j(t)}, \\ \Phi_j^{(2)}(t) &\equiv \left(\frac{\partial^2\Phi_j}{\partial t'^2}\right)_{t'=t_j(t)} = [\mathbf{a}_s \cdot \mathbf{k}_j^s + (\mathbf{v}_s \cdot \nabla_s)(\mathbf{k}_j^s \cdot \mathbf{v}_s)]_{t'=t_j(t)}, \end{aligned} \tag{6.26}$$

where $\mathbf{a}_s = \dot{\mathbf{v}}_s$ is the source acceleration, the frequency derivatives of Φ_j are again only with respect to explicit ω dependence, and all quantities are to be evaluated at observation time t according to the above two mappings. In the second line of Eq. (6.25), the quantities $A_j(t)e^{i\Phi_j(t)}$ are just the Green function components with arguments evaluated according to these mappings. The additional factor $e^{i(\omega_j(t)-\omega_0)[t-t_j(t)]}$ produces a phase correction due to the variation of the time of flight with source motion, and the numerator $\mathcal{N}_j(t)$ generates a weighting correction according to the rate of change of the Doppler effect with time. Although not obvious from Eq. (6.26), it is indeed the case that $\mathcal{N}_j \to 1$ in the limit of vanishing source velocity so that Eq. (6.25) is consistent with Eq. (2.8) in the static limit. The narrow time window result (6.17) now takes the simple form

$$\mathcal{G}(t;\omega_0) \approx \sum_j g_j(t_0;\omega_0) e^{-i\Delta\omega_j^D(t_0)(t-t_0)}. \tag{6.27}$$

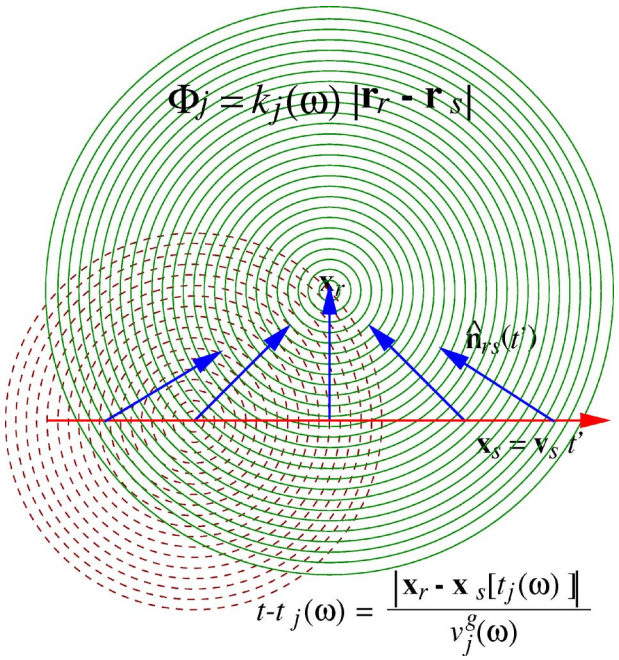

FIG. 4. (Color online) Illustration of range-independent case for the case of a horizontal, linear source trajectory. The horizontal wave fronts Φ_j for each mode are circular, and uniformly spaced, although the wave number $k_j(\omega)$ is a nontrivial function of frequency, determined by the eigenvalue equation (5.3). As in Fig. 3, a fictitious signal due to a stationary source (also with uniformly spaced, circular wave fronts) is used to illustrate the source-receiver time delay.

VII. RANGE INDEPENDENT CASE

We now consider various special cases in order to illustrate the general results. The simplest is the range-independent case, illustrated in Fig. 4, where the Green function takes the form (5.2). At high frequency the modes themselves have convenient amplitude-phase decomposition (5.5), and together with the asymptotic expansion for the Hankel function this leads to the ray formulation of the Doppler shift discussed in Sec. IV. However, even at low frequency, where the modes do not have a convenient sinusoidal structure, the horizontal dependence remains sinusoidal. The previous theory therefore allows a convenient formulation of the low-frequency Doppler shift, so long as the source velocity is horizontal. For large $|\mathbf{r}-\mathbf{r}'|$ we identify

$$\begin{aligned}\Phi_j &= k_j(\omega)|\mathbf{r}_r - \mathbf{r}_s|, \\ A_j &= \frac{1}{\rho(z_s)} \frac{\psi_j^*(z_s;\omega)\psi_j(z_r;\omega)}{\sqrt{-8\pi i k_j(\omega)|\mathbf{r}_r - \mathbf{r}_s|}}, \end{aligned} \tag{7.1}$$

and therefore

$$\mathbf{k}_j^r = -\mathbf{k}_j^s = k_j(\omega)\hat{\mathbf{n}}_{rs}, \tag{7.2}$$

where $\hat{\mathbf{n}}_{rs}=(\mathbf{r}_r-\mathbf{r}_s)/|\mathbf{r}_r-\mathbf{r}_s|$ is the horizontal unit vector pointing from source to receiver. No particular orthogonality properties of the mode eigenfunctions, which are basically "carried along for the ride," are assumed in what follows. Therefore, again, the results do not preclude more complicated physical situations, e.g., in which the acoustic medium is coupled to other elastic media. In order to obtain an analytically tractable problem, we consider the simple case of linear motion, $\mathbf{r}_s(t')=\mathbf{r}_s^0+\mathbf{v}_s t'$, choosing $\mathbf{v}_s=v\hat{\mathbf{x}}$ to be constant and along the x axis (Ref. [2] considers also the case of circular motion). We take $\lambda=1/k_j(\omega_0)$, and $\xi=|\mathbf{r}_r-\mathbf{r}_s^0|$ (since deviations from simple plane wave structure, which locally approximates the outgoing spherical wave, appear only on the scale of the separation distance), and hence $N=k_j(\omega_0)|\mathbf{r}_r-\mathbf{r}_s^0|$ and $\tau'=vt'/|\mathbf{r}_r-\mathbf{r}_s^0|$. The conditions for validity of the stationary phase approximation are therefore met so long as the separation is much larger than the wavelength. The phase function is

$$f_j = \gamma_j \frac{|\mathbf{r}_r-\mathbf{r}_s(\tau')|}{|\mathbf{r}_r-\mathbf{r}_s^0|} \tag{7.3}$$

and the first stationarity condition (6.6) takes the form

$$\zeta = \frac{\omega-\omega_0}{vk_j(\omega_0)} = \gamma_j \hat{\mathbf{n}}_{rs}(\tau_j)\cdot\hat{\mathbf{x}}, \tag{7.4}$$

where $\gamma_j(\omega)=k_j(\omega)/k_j(\omega_0)$. The solution to Eq. (7.4) is

$$\tau_j = \hat{n}_{rs}^x(0) - \frac{\zeta}{\sqrt{\gamma_j^2-\zeta^2}}|\hat{n}_{rs}^y(0)|, \tag{7.5}$$

whence $x_r-x_s(\tau_j)=\zeta|y_r-y_s^0|/\sqrt{\gamma_j^2-\zeta^2}$ and $|\mathbf{r}_r-\mathbf{r}_s(\tau_j)| =\gamma_j|y_r-y_s^0|/\sqrt{\gamma_j^2-\zeta^2}$ [where we have noted that since $\gamma_j>0$, ζ must have the same sign as $x_r-x_s(\tau_j)$]. The total phase takes the form

$$f_j+\zeta\tau_j = \zeta\hat{n}_{rs}^x(0) + \sqrt{\gamma_j^2-\zeta^2}|\hat{n}_{rs}^y(0)|, \tag{7.6}$$

in which the unit vector components are evaluated at $\tau'=0$. Since the acceleration term vanishes in this case, the second derivative (6.7) takes the form

$$f_j^{(2)} = \frac{(\gamma^2-\zeta^2)^{3/2}}{\gamma^2|\hat{n}_{rs}^y(0)|}, \tag{7.7}$$

and the final result is

$$\hat{\varphi}_j(\mathbf{x}_r;\omega) \approx \frac{i}{2\rho(z_s^0)k_j(\omega_0)v}\frac{\psi_j^*(z_s^0;\omega)\psi_j(z_r;\omega)}{\sqrt{\gamma_j^2-\zeta^2}} \times e^{ik_j(\omega_0)[\zeta(x_r-x_s^0)+\sqrt{\gamma_j^2-\zeta^2}|y_r-y_s^0|]}. \tag{7.8}$$

Although not obvious from the derivation, this final result turns out to be exact [1], even though Eq. (7.1) is only asymptotic.

The total phase for the second stationary phase computation may be put in the form

$$\tilde{f}_j = \frac{|\mathbf{r}_r-\mathbf{r}_s(\tau)|}{|\mathbf{r}_r-\mathbf{r}_s^0|}[\zeta\hat{n}_{rs}^x(\tau)+\sqrt{\gamma_j^2-\zeta^2}|\hat{n}_{rs}^y(\tau)|] \tag{7.9}$$

and the second stationarity condition (6.10) may be put in the form

$$\frac{\hat{n}_{rs}^x(\tau)}{|\hat{n}_{rs}^y(\tau)|} \equiv \cot|\theta_s| = \frac{\zeta_j-\gamma_j v/v_j^g}{\sqrt{\gamma_j^2-\zeta_j^2}}, \tag{7.10}$$

where $-\pi<\theta_s(\tau)\leqslant\pi$ is the angle between the source velocity and the instantaneous source-receiver separation vector [so that $\hat{n}_{rs}^x=\cos(\theta_s)$ and $\hat{n}_{rs}^y=\sin(\theta_s)$], and $v_j^g(\omega) =[\partial k_j(\omega)/\partial\omega]^{-1}$ is the mode group velocity. The same result may be obtained by directly by extremalizing (7.9) with respect to ζ. Note again that all frequency dependent quantities are to be evaluated at $\omega=\omega_j=\omega_0+k_j(\omega_0)v\zeta_j$. The inputs to the second derivative (6.11) are given by Eq. (7.7) and

$$v^2k_j(\omega_0)^2\partial_\omega^2 f_j = -\frac{|\hat{n}_{rs}^y(0)|(v/v_j^g)^2D_j}{\sqrt{\gamma_j^2-\zeta_j^2}},$$

$$\frac{d\tau_j}{d\zeta} = -|\hat{n}_{rs}^y(0)|\gamma_j\frac{\gamma_j-\zeta_j v/v_j^g}{(\gamma_j^2-\zeta_j^2)^{3/2}}, \tag{7.11}$$

where

$$D_j(\omega) \equiv k_j(\omega)\frac{\partial v_j^g(\omega)}{\partial\omega} \tag{7.12}$$

measures the rate of change of the group velocity relative to the phase velocity. One obtains

$$\tilde{f}_j^{(2)} = -\frac{|\hat{n}_{rs}^y(0)|}{\sqrt{\gamma_j^2-\zeta_j^2}}\left\{\left[\frac{\gamma_j-\zeta_j v/v_j^g}{\gamma_j^2-\zeta_j^2}\right]^2+(v/v_j^g)^2D_j\right\} = -\frac{|\hat{n}_{rs}^y(0)|}{\sqrt{\gamma_j^2-\zeta_j^2}[\hat{n}_{rs}^y(\tau)]^2}\left\{1-\left[\frac{v\hat{n}_{rs}^y(\tau)}{v_j^g}\right]^2(1-D_j)\right\}, \tag{7.13}$$

where the somewhat more transparent form in the second line follows from the real-time source-receiver direction,

$$[\hat{n}_{rs}^x(\tau),|\hat{n}_{rs}^y(\tau)|] = [\cos(\theta_s),\sin(\theta_s)] = \frac{(\zeta_j-\gamma_j v/v_j^g,\sqrt{\gamma_j^2-\zeta_j^2})}{\sqrt{[\gamma_j-\zeta_j v/v_j^g]^2+(\gamma_j^2-\zeta_j^2)[v/v_j^g]^2}}, \tag{7.14}$$

which in turn follows directly from Eq. (7.10). The result (7.13) also follows directly from computing the second

derivative of Eq. (7.9) with respect to ζ and evaluating it at $\zeta_j(\tau)$, which provides a useful check on the general theory. The time domain field (6.14) now follows in the form

$$\varphi_j(\mathbf{x}_r,t) \approx \frac{i}{2\rho(z_s^0)} e^{-i\omega_0 t}\psi_j^*[z_s^0;\omega_j(\tau)]\psi_j[z_r;\omega_j(\tau)] \times \frac{1}{\mathcal{N}_j(\tau)} e^{ik_j(\omega_0)|\mathbf{r}_r-\mathbf{r}_s(\tau)|[\zeta_j\hat{n}_{rs}^x(\tau)+\sqrt{\gamma_j^2-\zeta_j^2}|\hat{n}_{rs}^y(\tau)|]}, \tag{7.15}$$

with squared normalization,

$$\mathcal{N}_j(\tau)^2 = 2\pi i k_j(\omega_0)|\mathbf{r}_r-\mathbf{r}_s(\tau)|\frac{\zeta_j-\gamma_j v/v_j^g}{\cos(\theta_s)} \times\{1-[\sin(\theta_s)v/v_j^g]^2(1-D_j)\}. \tag{7.16}$$

The result (7.15) is identical to that obtained by Hawker [1]. He dealt explicitly only with the case of a stationary receiver, but it is actually a trivial step to substitute a time-dependent receiver position $\mathbf{x}_r(t)$ into his results to obtain the more general result given below.

The implicit dependence of the frequency ω_j on $\zeta_j(\tau)$ precludes a general analytic solution of the stationarity condition (7.10). However, for small source velocity one may generate a solution as a power series in the small parameter $\epsilon_j = v/v_j^g(\omega_0)$,

$$\zeta_j = \zeta_{j,0} + \epsilon_j\zeta_{j,1} + \epsilon_j^2\zeta_{j,2} + \cdots,$$

$$\gamma_j = \gamma_{j,0} + \epsilon_j\gamma_{j,1} + \epsilon_j^2\gamma_{j,2} + \cdots,$$

$$\tilde{f}_j = \frac{|\mathbf{r}_r-\mathbf{r}_s(\tau)|}{|\mathbf{r}_r-\mathbf{r}_s^0|}(f_{j,0} + \epsilon_j f_{j,1} + \epsilon_j^2 f_{j,2} + \cdots), \tag{7.17}$$

in which the coefficients are given by [1]

$$\zeta_{j,0} = \gamma_{j,1} = f_{j,1} = \cos(\theta_s),$$

$$\zeta_{j,1} = \gamma_{j,0} = f_{j,0} = 1,$$

$$\zeta_{j,2} = \frac{1}{2}\cos(\theta_s)\{1+(1-D_{j,0})[1+\sin^2(\theta_s)]\},$$

$$\gamma_{j,2} = \frac{1}{2}[2-D_{j,0}\cos^2(\theta_s)],$$

$$f_{j,2} = \frac{1}{2}[1+(1-D_{j,0})\cos^2(\theta_s)], \tag{7.18}$$

where $D_{j,0}=D_j(\omega_0)$. Correct to *first order* in ϵ_j one therefore obtains $\mathcal{N}_j=\sqrt{2\pi i k_j(\omega_0)|\mathbf{r}_r-\mathbf{r}_s(\tau)|}$.

To illustrate, using $\omega_0=2\pi\times 100$ Hz, $v_j^g \simeq c=1500$ m/s, $v=5$ m/s, one obtains $k_j(\omega_0)\sim\omega_0/c\simeq 0.4$ m^{-1} and $\epsilon_j = 1/300$. Thus the stationary phase approximation, requiring $k_j(\omega_0)|\mathbf{r}_r-\mathbf{r}_s| \gg 1$, will be valid for separations larger than, say, a few tens of meters. The approximation will therefore be extremely accurate for the more typical separations of order kilometers. On the other hand, $k_j(\omega_0)\epsilon_j \sim 10^{-3}$ m^{-1} implies that first order contributions to the phase $N\tilde{f}_j$ will be of order unity for separations of order a kilometer or greater. Similarly, $k_j(\omega_0)\epsilon_j^2 \sim 3\times 10^{-6}$ m^{-1}, $k_j(\omega_0)\epsilon_j^3 \sim 10^{-8}$ m^{-1} implies that second order corrections become important for separations of order 300 km or greater, while third order corrections may be dropped for separations less than 10^5 km. Clearly, including zeroth and first order corrections alone should suffice for most applications.

In the neighborhood of some reference time t_0 one obtains

$$N\tilde{f}_j(\zeta_j(t_0),t_0) = k_j(\omega_0)|\mathbf{r}_r(t_0)-\mathbf{r}_s(t_0)| \times\left[1+\frac{\hat{\mathbf{n}}_{rs}(t_0)\cdot\mathbf{v}_s}{v_j^g(\omega_0)}+O(\epsilon_j^2)\right], \tag{7.19}$$

and the frequency Doppler shift is given by

$$\begin{aligned}\Delta\omega_j^D(t_0) &= k_j(\omega_0)\frac{d}{dt}[|\mathbf{r}_r(t)-\mathbf{r}_s(t)|\tilde{f}_j(\zeta_j(t),t)]_{t=t_0}\\ &= k_j(\omega_0)[\zeta_j(v_r^x-v_s)+\sqrt{\gamma_j^2-\zeta_j^2}v_r^y]_{t=t_0}\\ &= k_j(\omega_0)\hat{\mathbf{n}}_{rs}(t_0)\cdot(\mathbf{v}_r-\mathbf{v}_s)[1+O(\epsilon_j)].\end{aligned} \tag{7.20}$$

The parameters appearing in the time domain signal (6.17) in the neighborhood of t_0 are therefore given by (keeping only leading corrections):

$$\omega_j^D(t_0) = \omega_0 + k_{j,0}\hat{\mathbf{n}}_{rs}(t_0)\cdot(\mathbf{v}_s-\mathbf{v}_r),$$

$$B_j(t_0) \equiv \frac{1}{\rho(z_s^0)}\psi_j^*[z_s^0;\omega_j(t_0)]\psi_j[z_r(t_0);\omega_j(t_0)] \times\frac{e^{ik_j(\omega_0)|\mathbf{r}_r(t_0)-\mathbf{r}_s(t_0)|[1+\hat{\mathbf{n}}_{rs}(t_0)\cdot\mathbf{v}_s/v_j^g(\omega_0)]}}{\sqrt{-8\pi i k_{j,0}|\mathbf{r}_r(t_0)-\mathbf{r}_s(t_0)|}},$$

$$\omega_j(t_0) = \omega_0 + k_{j,0}\hat{\mathbf{n}}_{rs}(t_0)\cdot\mathbf{v}_s. \tag{7.21}$$

An illustrative numerical solution is described in Fig. 5. Note that an equivalent approximate result, Eq. (22) in Ref. [4], appears to differ in a number of ways from the rigorous result (7.21). When examined closely, however, the differences are minor. First, these authors evaluate k_j at the Doppler shifted (receiver) frequency ω_j^D, rather than the source frequency ω_0. As a result, $\mathbf{v}_r$ replaces $\mathbf{v}_s$ in the $[1+\hat{\mathbf{n}}_{rs}(t_0)\cdot\mathbf{v}_s/v_j^g(\omega_0)]$ exponent correction factor in Eq. (7.19). When their k_j is reexpanded to first order about ω_0, the two velocities are interchanged and the discrepancy disappears. Second, they evaluate the mode eigenfunctions ψ_j at the same fully Doppler shifted receiver frequency, instead of the partially Doppler shifted (by source motion only) frequency $\omega_j(t_0)$. With this replacement, the prefactor $B_j(t_0)$ is correct only to zeroth order in ϵ_j, and is therefore accurate only if the eigenfunctions vary weakly with frequency. Under most circumstances this is probably a reasonable assumption, and one may, for increased numerical efficiency, simply set $\omega_j(t_0)=\omega_0$ (or ω_j^D) inside the mode eigenfunctions. However, care should be taken for modes close to the boundary between discrete and continuous spectrum where more rapid dependence on frequency occurs [5,6]. Finally, the sinusoidal

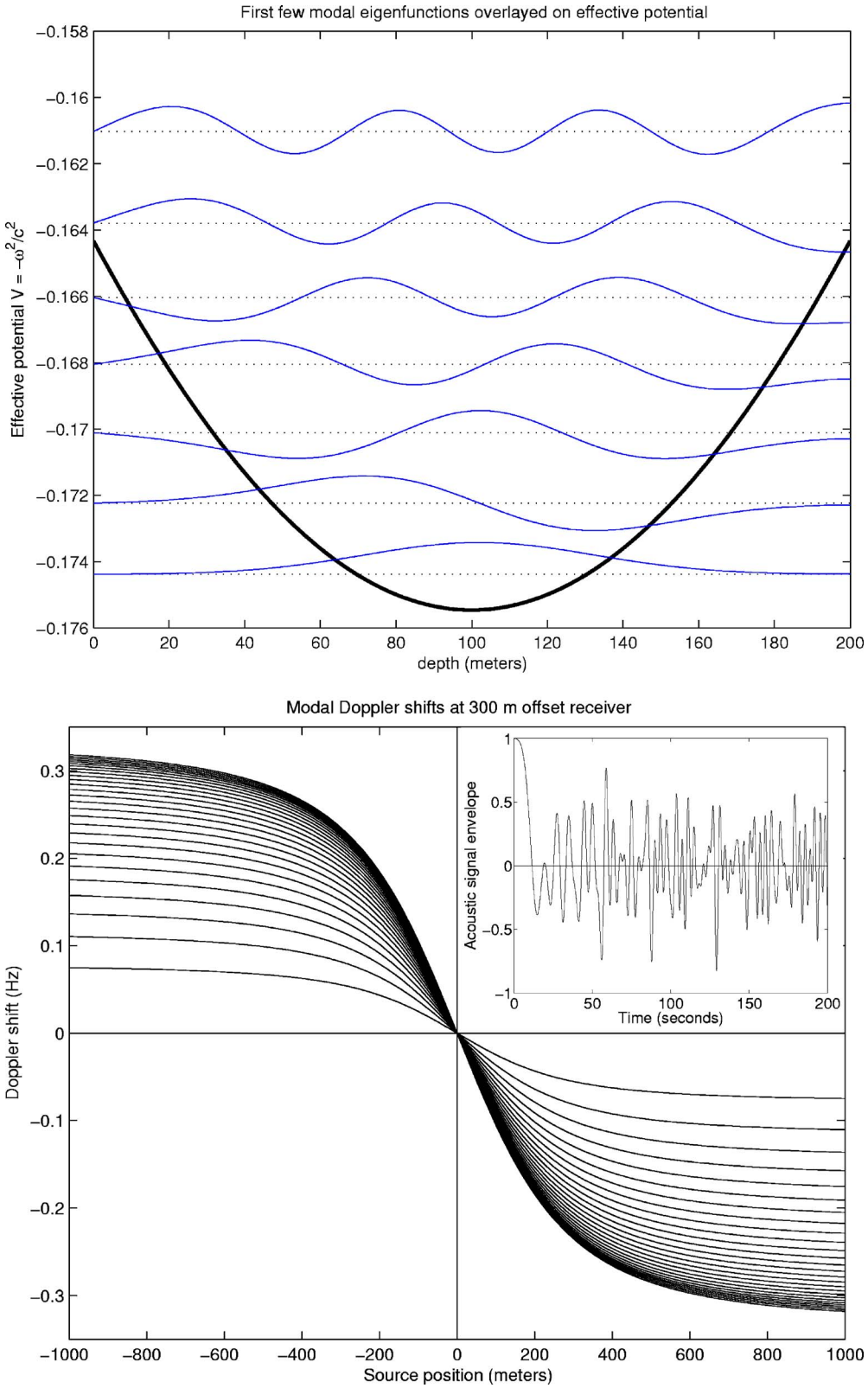

FIG. 5. (Color online) Illustration of modal Doppler shifts for the range-independent case using a parabolic sound speed profile $c(z)=c_0+c_1(2z/H_0+1)^2$ with $c_0=1500$ m/s, $c_1=50$ m/s, and vertical coordinate in the range $-H_0\leqslant z\leqslant 0$ with depth $H_0=200$ m. The density ρ is taken to be uniform. The source moves at speed $v_s=5$ m/s, depth $z=-H_0/2$, and has frequency $\omega_0=2\pi\times 100$ Hz. The receiver is taken to be fixed at the same depth at a perpendicular distance of $d_0=300$ m from the source track (see Fig. 4). The effective potential $V=-\omega^2/c^2$, overlayed by the first few modal eigenfunctions $\psi_j(z)$ (each offset by the corresponding eigenvalue $-k_j^2$ indicated by the dotted lines) is shown in the upper plot. The eigenfunctions are taken to obey Dirichlet (free surface) boundary conditions at $z=0$, and Neumann (rigid bottom) boundary conditions at $z=-H_0$. The leading order Doppler shifts $\Delta\omega_j^D/2\pi=-k_j(\omega_0)v_s x/2\pi\sqrt{x^2+d_0^2}$ [Eq. (7.21)] as functions of the distance x along the track, are shown in the lower plot for all propagating modes (for which $k_j^2>0$—the first 27 modes in this case). The inset shows the signal envelope Re $\phi(\mathbf{x}_r,t)$ (carrier tone $e^{-i\omega_0 t}$ removed), normalized to unity at $x=t=0$, as the source traverses the positive part of the track, $0\leqslant x\leqslant 1$ km. The chaotic beating phenomena is due to mode interference.

"window function" is replaced by $\delta(\omega-\omega_j^D)$, which is only valid for very large Δt.

The group velocity and its frequency derivative, required as inputs to the above results, may be computed directly from the mode eigenfunctions. The required relations are summarized in Appendix A.

VIII. ADIABATIC APPROXIMATION

A. Adiabatic Green function

The adiabatic approximation, in which scattering of energy between local modes is ignored, is commonly used for the frequency-domain Green function in the case of weakly

range-dependent media. Let ξ be the scale of horizontal variation of c and ρ, and let $\mathbf{R}=\mathbf{r}/\xi$. The approximation is derived in the limit of large ξ by seeking solutions to the source-free acoustic equation in the form

$$\phi(z;\mathbf{r}) = A(z;\mathbf{R})e^{i\xi\varphi(\mathbf{R})}, \tag{8.1}$$

in which the amplitude A has a multiple scales expansion in inverse powers of ξ:

$$A(z;\mathbf{R}) = A_0(z;\mathbf{R}) + \frac{1}{\xi}A_1(z;\mathbf{R}) + \frac{1}{\xi^2}A_2(z;\mathbf{R}) + \cdots . \tag{8.2}$$

Substituting this form into Eq. (2.2), one obtains at zeroth order in ξ:

$$\left(\rho\partial_z\frac{1}{\rho}\partial_z + \frac{\omega^2}{c^2}\right)A_0 = |\nabla_{\mathbf{R}}\varphi|^2 A_0. \tag{8.3}$$

This is an eigenvalue equation for the z dependence of A_0, with eigenvalue $|\nabla_{\mathbf{R}}\varphi|^2$. The solutions are therefore given by

$$A_0 = \mathcal{A}_0(\mathbf{R})\psi_j(z;\mathbf{r})$$

$$|\nabla_{\mathbf{R}}\varphi|^2 = k_j(\mathbf{r})^2, \tag{8.4}$$

in which $\mathcal{A}_0$ is an as yet undetermined amplitude, which for the acoustic problem may be normalized be making ψ_j real. The Eikonal equation obeyed by φ implies that it is determined by Fermat's principle:

$$\begin{aligned}\xi\varphi(\mathbf{R}) \equiv \Phi_j(\mathbf{r}_r,\mathbf{r}_s;\omega) &= \int_0^s k_j[\mathbf{r}(s')]ds' \\ &\approx k_j(\mathbf{r}_s)|\mathbf{r}_s-\mathbf{r}_r|, \quad |\mathbf{r}_s-\mathbf{r}_r| \ll \xi,\end{aligned} \tag{8.5}$$

in which the integration path $\mathbf{r}(s')$, parametrized by arc length and with given endpoints $\mathbf{r}(0)=\mathbf{r}_s$ and $\mathbf{r}(s)=\mathbf{r}_r$, is that which minimizes Φ_j and is the solution to the pair of recursion relations

$$\frac{d\mathbf{r}(s')}{ds'} = \hat{\mathbf{n}}(s'),$$

$$\begin{aligned}\frac{d\hat{\mathbf{n}}(s')}{ds'} &= [\mathbb{1}-\hat{\mathbf{n}}(s')\hat{\mathbf{n}}(s')]\cdot\nabla\ln\{k_j[\omega;\mathbf{r}(s')]\} \\ &= \hat{\mathbf{m}}(s')[\hat{\mathbf{m}}(s')\cdot\nabla]\ln\{k_j[\mathbf{r}(s')]\},\end{aligned} \tag{8.6}$$

in which $\hat{\mathbf{n}}(s')$ is the unit vector tangent to the ray at $\mathbf{r}(s')$, and $\hat{\mathbf{m}}(s')\equiv[\hat{n}_y(s'),-\hat{n}_x(s')]$ is the corresponding normal. The last line of Eq. (8.6) demonstrates that horizontal refraction occurs in the presence of a gradient in k_j in the direction orthogonal to the ray.

At first order in ξ^{-1} one obtains

$$\begin{aligned}\left[\rho\partial_z\frac{1}{\rho}\partial_z + \frac{\omega^2}{c^2} - k_j(\mathbf{r})^2\right]A_1 &= 2i\sqrt{\rho}\mathcal{A}_0\nabla_{\mathbf{R}}\varphi\cdot\nabla_{\mathbf{R}}\frac{\psi_j}{\sqrt{\rho}} \\ &\quad + i(2\nabla_{\mathbf{R}}\varphi\cdot\nabla_{\mathbf{R}}\mathcal{A}_0 + \nabla_{\mathbf{R}}^2\varphi)\mathcal{A}_0\psi_j.\end{aligned} \tag{8.7}$$

Since, as a function of z for each fixed $\mathbf{R}$, ψ_j is the kernel of the operator on the left hand side of Eq. (8.6), in order for a solution to exist, the right hand side must be orthogonal to ψ_j. Multiplying by ψ_j/ρ and integrating over z, this condition determines $\mathcal{A}_0$ via

$$\nabla_{\mathbf{R}}\varphi\cdot\nabla_{\mathbf{R}}\ln(\mathcal{A}_0) = -\frac{1}{2}\nabla_{\mathbf{R}}^2\varphi, \tag{8.8}$$

where we have used the fact that $2\int dz(\psi_j/\sqrt{\rho})\nabla_{\mathbf{R}}(\psi_j/\sqrt{\rho}) = \nabla_{\mathbf{R}}\int dz\psi_j^2/\rho = 0$ due to the normalization of ψ_j. The solution is

$$\begin{aligned}\mathcal{A}_{0,j}(\mathbf{r}_r,\mathbf{r}_s;\omega) \equiv \mathcal{A}_0(\mathbf{R}) &= \lim_{s_0\to 0}\frac{1}{\sqrt{k_j(\mathbf{r}_s)s_0}} \\ &\quad\times\exp\left\{-\frac{1}{2}\int_{s_0}^s ds'\frac{\nabla_{\mathbf{r}}^2\Phi_j[\mathbf{r}(s'),\mathbf{r}_s;\omega]}{k_j[\mathbf{r}(s')]}\right\} \\ &\approx \frac{1}{\sqrt{\Phi_j(\mathbf{r}_r,\mathbf{r}_s;\omega)}}, \quad k_j(\mathbf{r}_s)^{-1} \ll |\mathbf{r}_r-\mathbf{r}_s| \ll \xi\end{aligned} \tag{8.9}$$

in which the prefactor in the second line eliminates the logarithmic singularity in the exponent as $s_0\to 0$. Evaluation of $\nabla^2\Phi_j$ requires a second pair of recursion relations. Let $\boldsymbol{\rho}(s')=(d\mathbf{r}/d\theta)_\Phi$ and $\boldsymbol{\nu}(s')=(d\hat{\mathbf{n}}/d\theta)_\Phi$ be the rate of change of ray coordinate and unit normal, on the fixed level curve of Φ_j defined by $\mathbf{r}(s')$, with initial ray direction θ (defined by $\hat{\mathbf{n}}(0)=[\cos(\theta),\sin(\theta)]$). Then $\boldsymbol{\rho}(s)=\rho(s)\hat{\mathbf{m}}(s)$, $\boldsymbol{\nu}(s)=\nu(s)\hat{\mathbf{m}}(s)$ are both parallel to the level curve of Φ_j, and the magnitudes $\rho(s')$ and $\nu(s')$ obey the recursion relations

$$\frac{d\rho(s')}{ds'} = \nu(s'),$$

$$\begin{aligned}\frac{d\nu(s')}{ds'} &= -\rho(s')k_j[\mathbf{r}(s')]\hat{\mathbf{m}}(s')\cdot\left\{[\hat{\mathbf{m}}(s')\cdot\nabla]\nabla\frac{1}{k_j[\mathbf{r}(s')]}\right\} \\ &\quad -\nu(s')[\hat{\mathbf{n}}(s')\cdot\nabla]\ln\{k_j[\mathbf{r}(s')]\}.\end{aligned} \tag{8.10}$$

with initial conditions $\rho(0)=0$ and $\nu(0)=1$. Then

$$\frac{k_j[\mathbf{r}(s')]\nu(s')}{\rho(s')} = \hat{\mathbf{m}}(s')\cdot\{[\hat{\mathbf{m}}(s')\cdot\nabla]\nabla\Phi_j(\mathbf{r}(s'),\mathbf{r}_s;\omega)\} \tag{8.11}$$

is the curvature of the level curve of Φ_j at $\mathbf{r}(s')$. On the other hand, the second normal derivative may obtained directly from Eq. (8.6) via

$$\begin{aligned}(\hat{\mathbf{n}}(s')\cdot\nabla)\nabla\Phi_j[\mathbf{r}(s'),\mathbf{r}_s;\omega] &= \frac{d}{ds'}\{k_j[\mathbf{r}(s')]\hat{\mathbf{n}}(s')\} \\ &= \nabla k_j(\mathbf{r}(s'))).\end{aligned} \tag{8.12}$$

Thus using

$$\begin{aligned}\nabla^2\Phi_j(s') &= \hat{\mathbf{n}}(s')\cdot\{[\hat{\mathbf{n}}(s')\cdot\nabla]\nabla\Phi_j(s')\} \\ &\quad + \hat{\mathbf{m}}(s')\cdot\{[\hat{\mathbf{m}}(s')\cdot\nabla]\nabla\Phi_j(s')\},\end{aligned} \tag{8.13}$$

one finally obtains

$$\mathcal{A}_{0,j}(\mathbf{r}_r,\mathbf{r}_s;\omega) = \lim_{s_0\to 0} \frac{1}{\sqrt{k_j(\mathbf{r}_r)s_0}} \exp\left[-\int_{s_0}^{s} ds' \frac{\nu(s')}{2\rho(s')} \right]. \tag{8.14}$$

Combining Eq. (8.9), valid for large Φ_j, with the range-independent result (5.2), valid for $|\mathbf{r}_r-\mathbf{r}_s| \ll \xi$, one finally obtains the Green function

$$\hat{G}(\mathbf{x}_r,\mathbf{x}_s;\omega) \approx \frac{i}{4\rho(z_s)} \sum_j \psi_j(z_s;\omega;\mathbf{r}_s)\psi_j(z_r;\omega;\mathbf{r}_r) \times \mathcal{H}_j(\mathbf{r}_r,\mathbf{r}_s;\omega), \tag{8.15}$$

in which

$$\mathcal{H}_j(\mathbf{r}_r,\mathbf{r}_s;\omega) = \begin{cases} H_0^{(1)}[\Phi_j(\mathbf{r}_r,\mathbf{r}_s;\omega)], \\ |\mathbf{r}_r-\mathbf{r}_s| \ll \xi \\ \sqrt{\dfrac{2}{i\pi}}\mathcal{A}_{0,j}(\mathbf{r}_r,\mathbf{r}_s;\omega)e^{i\Phi_j(\mathbf{r}_r,\mathbf{r}_s;\omega)}, \\ |\mathbf{r}_r-\mathbf{r}_s| \gg k_j(\mathbf{r}_s)^{-1}. \end{cases} \tag{8.16}$$

All higher order terms, which induce scattering between modes, in the expansion (8.2) have been neglected.

B. Doppler theory

Comparing the structure of the adiabatic Green function (8.15) with the form (6.3) imposed by the general theory, one immediately identifies

$$\Phi_j(\mathbf{x}_r,\mathbf{x}_s;\omega) = \Phi_j(\mathbf{r}_r,\mathbf{r}_s;\omega),$$

$$A_j(\mathbf{x}_r,\mathbf{x}_s;\omega) = \frac{\psi_j(z_s;\omega;\mathbf{r}_s)\psi_j(z_r;\omega;\mathbf{r}_r)}{\rho(z_s)\sqrt{-8\pi i}}\mathcal{A}_{0,j}(\mathbf{r}_r,\mathbf{r}_s;\omega), \tag{8.17}$$

where in the adiabatic case the dependence of the phase is on the horizontal coordinates alone. The adiabatic condition $k_j(\mathbf{r}_s)\xi \gg 1$ is seen to be identical to the general requirement (1.4) for a well defined Doppler shift, and no further constraints need to be imposed.

The local wave vectors (6.4) are given by

$$\mathbf{k}_j^r(\mathbf{r}_r,\mathbf{r}_s;\omega) = k_j(\omega;\mathbf{r}_r)\hat{\mathbf{n}}_j^r,$$

$$\mathbf{k}_j^s(\mathbf{r}_r,\mathbf{r}_s;\omega) = -k_j(\omega;\mathbf{r}_s)\hat{\mathbf{n}}_j^s, \tag{8.18}$$

in which the unit vectors $\hat{\mathbf{n}}_j^{s,r} = [d\mathbf{r}(s')/ds']_{s'=0,s}$ are the horizontal directions at source and receiver defined by the ray path connecting them.

A common form of the adiabatic approximation is based on the assumption that horizontal variations in the k_j, in addition to being slow, are bounded and small. In this case one may approximate the ray path by a straight line to obtain

$$\Phi_j(\mathbf{r}_r,\mathbf{r}_s;\omega) = \int_0^{|\mathbf{r}_r-\mathbf{r}_s|} k_j(\omega;\mathbf{r}_s+s'\hat{\mathbf{n}}_{rs})ds', \tag{8.19}$$

in which $\hat{\mathbf{n}}_{rs}$ is the unit vector pointing from source to receiver. The contours of constant Φ_j are near circular, and ray bending (horizontal refraction) is neglected [4]. The local wave vectors are now given by Eq. (8.18) with $\hat{\mathbf{n}}_j^{r,s}$ both replaced by $\hat{\mathbf{n}}_{rs}$. In deep ocean environments, where the propagating modes are confined within the SOFAR channel, this approximation is generally valid. However, in littoral environments, where the modes are much more sensitive to bathymetric variations, it is likely to break down. When there are slow, large scale variations in the depth, the horizontal wavenumber $k_j(\mathbf{r})$, along with the horizontal mode group velocity, may change by factors of order unity. This will induce significant ray bending, and the full ray theory must be employed to compute Φ_j. For example, a ray propagating shorewards into increasingly shallow water will eventually encounter a turning point where k_j vanishes, causing it to reflect back towards deeper water again [3].

The first stationarity condition (6.6) for $\tau' = \tau_j(\zeta)$ takes the form

$$\zeta/\lambda = -\hat{\mathbf{u}}\cdot\mathbf{k}_j^s(\mathbf{r}_r,\mathbf{r}_s^0+\hat{\mathbf{v}}\xi\tau_j;\omega_0+v\zeta/\lambda), \tag{8.20}$$

where we take $\mathbf{r}_s = \mathbf{r}_s^0 + \mathbf{v}_s t'$, with constant velocity $\mathbf{v}_s = v\hat{\mathbf{u}}$ in some horizontal direction $\hat{\mathbf{u}}$. Equation (8.20) determines the time (or times, since multiple solutions are not forbidden in principle) $t' = \xi\tau_j/v$, in the source's frame of reference, at which a specified Doppler shift $v\zeta/\lambda = -\mathbf{k}_j^s\cdot\mathbf{v}_s$ occurs. Solution of this equation requires detailed knowledge of the phase function Φ_j, and in general must be carried out numerically, though analytic solutions are possible for simple model forms for $k_j(\omega;\mathbf{r})$ (e.g., constant plus linear gradient). In the linear ray approximation (8.19), one obtains $\mathbf{k}_j^s(\mathbf{r}_r,\mathbf{r}_s;\omega) \approx -k_j(\omega;\mathbf{r}_s)\hat{\mathbf{n}}_{rs}$, and Eq. (8.20) simplifies to

$$\zeta = -\lambda k_j[\omega+v\zeta/\lambda;\mathbf{r}_s(\tau_j)]\hat{\mathbf{u}}\cdot\hat{\mathbf{n}}_{rs}(\tau_j), \tag{8.21}$$

which still in general requires a numerical solution. Here $\hat{\mathbf{n}}_{rs}(\tau_j)$ is the source-receiver direction at source time τ_j. In the range-independent case (8.21) reduces to Eq. (7.4) [with the choice $\lambda = k_j(\omega_0)$].

In the adiabatic approximation the second stationarity condition (6.10) takes the form

$$\tau - \tau_j(\zeta_j) = \frac{v}{\xi}\left(\frac{\partial\Phi_j}{\partial\omega}\right)_{\omega=\omega_0+v\zeta_j/\lambda} = \frac{v}{\xi}\int_0^s \frac{ds'}{v_j^g[\omega_0+v\zeta_j/\lambda;\mathbf{r}(s')]}, \tag{8.22}$$

with $\mathbf{r}(0) = \mathbf{r}_s(\tau_j)$ and $\mathbf{r}(s) = \mathbf{r}_r$, and with local group velocity $v_j^g(\omega;\mathbf{r}) = [\partial k_j(\omega;\mathbf{r})/\partial\omega]^{-1}$. The left hand side is clearly the (scaled) time of flight, determined by the local group velocity along the ray path.

Given the solution $\tau' = \tau_j(\zeta)$ of Eq. (8.20), the *forward* calculation, via Eq. (8.22), of the arrival time $\tau = \tau(\zeta,\tau_j)$, is trivial: one need only evaluate the scaled flight time for the given values of ζ and $\tau_j(\zeta)$, and add it to $\tau_j(\zeta)$. Therefore, for numerical purposes, it is probably most efficient to solve for the measured signal *parametrically* by plotting

$\varphi_j[\mathbf{r}_r, \xi\tau(\zeta)/v]$ against $\tau(\zeta)$, both as a function of scaled Doppler shift ζ. There is a complication when the receiver coordinate $\mathbf{r}_r = \mathbf{r}_r(\xi\tau/v)$ becomes time dependent, because τ now appears implicitly in the upper limit of the time of flight integral. Even the forward calculation then requires an iterative solution that matches the value of τ computed on the left hand side of Eq. (8.22) with the value used to determine the receiver position on the right hand side. One could instead, in principle, solve Eq. (8.20) for the Doppler shift as a function of source time $\zeta = \zeta_j(\tau')$, then solve Eq. (8.22) for $\tau(\zeta_j, \tau')$ as before, and thereby determine the receiver signal $\varphi_j\{\mathbf{r}_r, \xi\tau[\zeta_j(\tau')]/v\}$ parametrically as a function of retarded time τ' [2,3]. However, inversion of Eq. (8.20) is probably rather difficult since a new diagonalization of the mode equation would have to be performed for each iteration in the search for the correct ζ.

Equations (8.20) and (8.22) determine the full Doppler shift (6.15). The phase and amplitude, for input into Eqs. (6.14) and (6.17), evaluated at the correct Doppler shifted frequency, follow from Eq. (8.17). Finally, to completely specify all inputs into these two equations, one requires now only the terms for computing the second derivatives $f_j^{(2)}$ and $\tilde{f}_j^{(2)}$ given by Eqs. (6.7) and (6.11). The relevant expressions are provided in Appendix B.

In Ref. [4] a heuristic form for the adiabatic Doppler shift is given which differs substantially from the rigorous result above. The most significant differences, in addition to those already discussed above for the range-independent case, are the neglect of corrections to the linear ray assumption (8.19) (thereby neglecting any nonradial components of the local wave vectors), and the appearance of group velocities evaluated only at the integration endpoints rather than the line average (8.22). In many applications the total variation in the mode structure across the region of interest is only a few percent, and these discrepancies are in fact very small. In more complicated cases, where there are gradual, but order unity relative variations in the bathymetry or in the sound speed profile, the full theory presented here must be used.

IX. SUMMARY AND CONCLUSIONS

Equations (6.14)–(6.18) are the basic results of this paper. It is worth summarizing their key ingredients and how each would be implemented in data processing:

(1) The basic assumption underlying the theory is the existence of the decomposition (6.3) of the Green function. Ray theory, range-independent mode theory, and weakly range-dependent adiabatic mode theory provide different limits in which this expansion may be realized explicitly. The validity of the adiabatic approximation is guided by precisely the same $\lambda/\xi \ll 1$ requirement that constrains the Doppler theory. Therefore, at least locally, the adiabatic approximation contains all necessary ingredients for a general Doppler shift calculation. Globally, however, things may be more complicated. As illustrated in Fig. 6, there may be regions, that could in fact separate source and receiver, where the adiabatic approximation fails. The full Green function must therefore tie together the different adiabatic regions, and

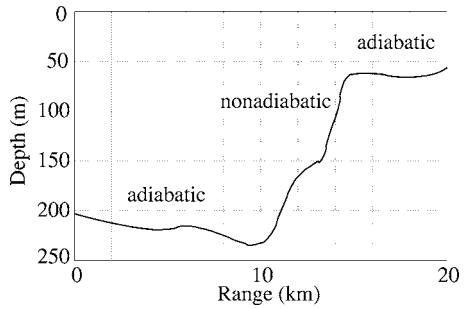

FIG. 6. Schematic example showing a shelflike topography which produces two adiabatic regions separated by a strongly scattering, nonadiabatic region. A source on the left will produce well defined Doppler frequencies at a receiver on the right (and vice versa) even though the phase functions $\Phi_j(\mathbf{x}_s, \mathbf{x}_r; \omega)$ may not exist, or at least fail to generate the required slowly varying wave vectors $\mathbf{k}_j^r$, $\mathbf{k}_j^s$, along the entire line joining $\mathbf{x}_r$ and $\mathbf{x}_s$.

hence the different pieces of the phase functions Φ_j, generalizing Eq. (8.15) to the case where $\mathbf{r}_r$ and $\mathbf{r}_s$ lie in different regions. This will require not only generalization of the horizontal dependence (8.16), but also allow for coupling, $\mathcal{A}_{ij}\psi_i(z;\omega;\mathbf{r}_s)\psi_j(z;\omega;\mathbf{r}_r)$, between different modes induced by rapid environmental changes in the intervening regions. Standard numerical codes, such as KRAKEN [9], already account for these mode coupling effects in various approximations, and could be used to compute the "scattering coefficients" $\mathcal{A}_{ij}$. One could then construct the proper generalization of Eq. (8.15), allowing direct application of the general results of Sec. VI. This will be investigated in detail in future work [16].

(2) In a similar vein, dissipation effects, appearing through an additional linear time derivative term in Eq. (2.1), and hence an additional $i\omega$ term in Eq. (2.2), will lead to complex mode eigenvalues, and in general alter the mode shapes. The Green function will decay exponentially with horizontal distance on some new frequency-dependent dissipation length scale $\xi_d(\omega)$, but with $\lambda/\xi_d \ll 1$ expected for most applications. These new features will strongly affect the computation of the amplitudes A_j (though probably less so the phases Φ_j) on scales larger than ξ_d. However, the existence of the decomposition (6.3), and the general theory that follows, should not be affected.

(3) Each Φ_j defines a pair of frequency-dependent local wave vectors $\mathbf{k}_j^r$, $\mathbf{k}_j^s$ [which reduce, after dividing by frequency, to the slowness vectors (4.10) in the ray limit]. The Doppler analysis ties these, through the stationarity conditions, to the observed Doppler shift. By Fourier transforming over a suitably narrow time window (but wide enough that the Heisenberg uncertaintylike condition $\Delta t|\Delta\omega^D| > 2\pi$ holds), Eq. (6.18) represents the measured signal as a superposition of different Doppler shifts (corresponding to different classical arrival paths in the ray limit, or mode group arrivals in the mode picture), of the same underlying source signal $\hat{S}(\omega)$. If $\hat{S}(\omega)$ is very sharply peaked (with bandwidth smaller than the Doppler shifts), $\hat{\phi}_0$ will have a discrete spectrum of sharp peaks, one at each Doppler shifted frequency.

(4) The object of the receiver data processing is to invert for some set of unknown source and/or environmental pa-

rameters. If the source signal and the source and receiver trajectories are known, one may, for example, tune the environmental model to obtain best agreement between predicted and known data. Alternatively, given an accurate environmental model, one may invert for source data.

(5) It may be the case that the source signal is stochastic so that, say, the mean signal $\langle S_0(t)\rangle=0$ vanishes, and only the source cross correlation function $\sigma(t-t')=\langle S_0(t)S_0(t')\rangle$ [whose Fourier transform is the source power spectrum $\hat{\sigma}(\omega)$] is known. In this case the measured signal is also stochastic and Eq. (6.14) must be used to construct a relation between the data covariance $\Phi(t-t')=\langle \phi_0(t)\phi_0(t')\rangle$ [whose Fourier transform is the receiver power spectrum $\hat{\Phi}(\omega)$] and σ. This will be addressed in future work [17].

ACKNOWLEDGMENTS

The author has greatly benefitted from many helpful conversations with E. M. Lavely, H. Schmidt, and A. S. Willsky. The support of the DARPA Advanced Technology Office, through the Robust Passive Sonar program, Contract No. N00024-01-C-6318, is gratefully acknowledged.

APPENDIX A: SOME USEFUL RESULTS FROM MODE PERTURBATION THEORY

All inputs to Eqs. (7.16)–(7.18) may be computed from the mode theory. Standard perturbation theory [5,6] yields the change in the eigenvalue $\Delta(k_j^2)$ under a change $\Delta(\omega^2/c^2)$ in the sound speed term in Eq. (5.3) in the form

$$\Delta(k_j^2)=\int dz\psi_j^*(z)\Delta(\omega^2/c^2)\Psi_j(z), \tag{A1}$$

where $\Psi_j(z)$ is the perturbed eigenfunction, given to first order by

$$\Psi_j(z)=\psi_j(z)+\sum_{l(\neq j)}\frac{C_{lj}}{k_j^2-k_l^2}\psi_l(z)+\cdots,$$

$$C_{lj}\equiv\int dz\psi_l^*(z)\Delta(\omega^2/c^2)\psi_j(z), \tag{A2}$$

with normalization

$$\int dz\psi_l^*(z)\psi_j(z)=\delta_{lj} \tag{A3}$$

and the condition that the change in eigenfunction be orthogonal to the original:

$$\int dz\psi_j^*(z)[\Psi_j(z)-\psi_j(z)]=0. \tag{A4}$$

The special case of a perturbation given by a simple frequency shift $\omega=\omega_0+\Delta\omega$ one obtains $\Delta(\omega^2/c^2)=(2\omega_0+\Delta\omega)\Delta\omega/c^2$, whence

$$\psi_j(z;\omega_0+\Delta\omega)=\psi_j(z;\omega_0)+2\omega_0\Delta\omega\times\sum_{l(\neq j)}\frac{c_{lj}(\omega_0)}{k_j(\omega_0)^2-k_l(\omega_0)^2}\psi_l(z;\omega_0)+O(\Delta\omega^2),$$

$$k_j(\omega)^2=k_j(\omega_0)^2+c_{jj}(\omega_0)(2\omega_0+\Delta\omega)\Delta\omega+4\omega_0^2\Delta\omega^2\sum_{l(\neq j)}\frac{|c_{lj}(\omega_0)|^2}{k_j(\omega_0)^2-k_l(\omega_0)^2}+O(\Delta\omega^3),$$

$$c_{lj}(\omega_0)\equiv\int dz\frac{\psi_l^*(z;\omega_0)\psi_j(z;\omega_0)}{c(z)^2}, \tag{A5}$$

and exact expressions for the group velocity and its derivative follow in the form

$$v_j^g(\omega)=\frac{k_j(\omega)}{\omega c_{jj}(\omega)},$$

$$D_j(\omega)\equiv k_j(\omega)\frac{dv_j^g(\omega)}{d\omega}=1-\frac{1}{2}v_j^g(\omega)^2\frac{d^2}{d\omega^2}k_j(\omega)^2,$$

$$=1-v_j^g(\omega)^2\left[c_{jj}(\omega)+4\omega^2\sum_{l(\neq j)}\frac{|c_{lj}(\omega)|^2}{k_j(\omega)^2-k_l(\omega)^2}\right]. \tag{A6}$$

The expression for $\psi_j(z;\omega_0+\Delta\omega)$ in Eq. (A5) may also prove useful for computing the Doppler shifted eigenfunctions in Eq. (7.15), in place of recomputing them at each new frequency ω_j, though care should be taken to ensure that the frequency shift is indeed sufficiently small for each j.

Although the horizontal label $\mathbf{r}$ has been suppressed, the above results also yield the local parameter values required for input to the adiabatic results in Sec. VIII.

The above formulas rely on the orthonormality of the mode eigenfunctions. In more realistic models the acoustic medium is coupled to an elastic half space (the ocean subbottom). Extension of the normal mode method to this case is straightforward, but the mode eigenfunctions now acquire a vector character (due to the presence of both longitudinal and transverse polarizations in the elastic medium) and the above formulas must be suitably generalized.

APPENDIX B: PHASE SECOND DERIVATIVES IN THE ADIABATIC APPROXIMATION

In this appendix it is shown how to compute the phase second derivatives (6.7) and (6.11) using the ray tracing formalism. The source wave-vector derivative, which requires second derivatives of Φ_j, follows from Eqs. (8.11) and (8.12). Use is made of the symmetry of $\Phi_j(\mathbf{r}_r,\mathbf{r}_s)=\Phi_j(\mathbf{r}_s,\mathbf{r}_r)$ under interchange of source and receiver coordinates. Thus if $\bar{\mathbf{r}}(s')=\mathbf{r}(s-s')$ is the reverse path from receiver to source, then

$$\Phi(\mathbf{r}_r,\mathbf{r}_s)=\int_0^s k_j[\bar{\mathbf{r}}(s')]ds', \tag{B1}$$

while the tangent vector $\bar{\mathbf{n}}(s')=d\bar{\mathbf{r}}(s')/ds'=-\hat{\mathbf{n}}(s-s')$, and corresponding normal vector $\bar{\mathbf{m}}(s')=-\hat{\mathbf{m}}(s-s')$, are reversed. One therefore obtains from Eq. (8.12)

$$(\hat{\mathbf{n}}_j^s \cdot \nabla_s)\mathbf{k}_j^s(\mathbf{r}_r,\mathbf{r}_s;\omega) = -(\bar{\mathbf{n}}(s)\cdot\nabla_s)\mathbf{k}_j^s(\mathbf{r}_r,\mathbf{r}_s;\omega) = -\nabla_s k(\mathbf{r}_s). \tag{B2}$$

The orthogonal derivative along $\hat{\mathbf{m}}_j^s$ is obtained by defining the reverse path quantities $\bar{\rho}(s')$, $\bar{\nu}(s')$ via Eq. (8.10), but with all quantities replaced by their overbarred counterparts. One obtains from Eq. (8.11)

$$\hat{\mathbf{m}}_j^s \cdot [(\hat{\mathbf{m}}_j^s \cdot \nabla_s)\mathbf{k}_j^s(\mathbf{r}_r,\mathbf{r}_s;\omega)] = \bar{\mathbf{m}}(s)\cdot[(\bar{\mathbf{m}}(s)\cdot\nabla_s)\mathbf{k}_j^s(\mathbf{r}_r,\mathbf{r}_s;\omega)] = \frac{k_j(\mathbf{r}_s)\bar{\nu}(s)}{\bar{\rho}(s)}. \tag{B3}$$

Finally, the component of the derivative along $\hat{\mathbf{n}}_j^s$ is obtained from Eq. (B3) via the equality of the mixed partial derivatives:

$$\hat{\mathbf{n}}_j^s \cdot [(\hat{\mathbf{m}}_j^s \cdot \nabla_s)\mathbf{k}_j^s(\mathbf{r}_r,\mathbf{r}_s;\omega)] = \hat{\mathbf{m}}_j^s \cdot [(\hat{\mathbf{n}}_j^s \cdot \nabla_s)\mathbf{k}_j^s(\mathbf{r}_r,\mathbf{r}_s;\omega)] = -(\hat{\mathbf{m}}_j^s\cdot\nabla_s)k(\mathbf{r}_s). \tag{B4}$$

Equations (B2)–(B4) provide the required expressions for the four components of the derivatives of $\mathbf{k}_j^s$ using the local coordinate system provided by the natural unit vectors $\hat{\mathbf{n}}_j^s$ and $\hat{\mathbf{m}}_j^s$. The required components along the source velocity $\mathbf{v}_s$ follow from the identity $\mathbf{v}_s = (\hat{\mathbf{n}}_j^s\cdot\mathbf{v}_s)\hat{\mathbf{n}}_j^s + (\hat{\mathbf{m}}_j^s\cdot\mathbf{v}_s)\hat{\mathbf{m}}_j^s$.

The second derivative of the phase with respect to frequency follows from the following general formula. For any function $q(\mathbf{r};\omega)$, the frequency derivative of its integral along the ray path is given by

$$\frac{\partial}{\partial\omega}\int_0^s ds' q[\mathbf{r}(s');\omega] = \int_0^s ds'[\partial_\omega q + q\partial_\omega \mathbf{r}(s')\cdot\hat{\mathbf{m}}(\hat{\mathbf{m}}\cdot\nabla)\ln(q/k_j)], \tag{B5}$$

in which $\partial_\omega \mathbf{r}(s)$ accounts for the variation of the ray path with frequency. The last term vanishes when $q=k_j$, consistent with the stationarity condition on Φ_j [Eq. (8.5)], and confirms Eq. (8.22). From Eq. (8.22) one therefore obtains

$$\partial_\omega^2 f_j(\mathbf{r}_r,\mathbf{r}_s;\omega) = -\frac{\lambda}{\xi}\int_0^s ds'\left[\frac{\partial_\omega v_j^g - v_j^g\partial_\omega\mathbf{r}\cdot\hat{\mathbf{m}}(\hat{\mathbf{m}}\cdot\nabla)\ln(v_j^g k_j)}{(v_j^g)^2}\right]. \tag{B6}$$

Finally, the derivative of $\tau_j(\zeta)$ is given by

$$\frac{d\tau_j(\zeta)}{d\zeta} = -\left[\frac{1+\mathbf{v}_s\cdot\partial_\omega\mathbf{k}_j^s}{\mathbf{a}_s\cdot\mathbf{k}_j^s + (\mathbf{v}_s\cdot\nabla_s)\mathbf{k}_j^s\cdot\mathbf{v}_s}\right]_{\omega=\omega_0+v\zeta/\lambda}, \tag{B7}$$

in which

$$\partial_\omega\mathbf{k}_j^s(\mathbf{r}_r,\mathbf{r}_s;\omega) = \frac{\hat{\mathbf{n}}_j^s}{v_j^g(\omega;\mathbf{r}_s)} + k_j(\mathbf{r}_s)\partial_\omega\hat{\mathbf{n}}_j^s. \tag{B8}$$

All quantities are to be evaluated at the stationary point $\zeta=\zeta_j(\tau)$, $\mathbf{r}_s=\mathbf{r}_s^0+\hat{\mathbf{u}}\xi\tau_j(\zeta_j)$ at the end. In Appendix A it was shown how to compute the required inputs, namely the local group velocities and their frequency derivative, from the mode eigenfunctions.

[1] K. E. Hawker, J. Acoust. Soc. Am. **65**, 675 (1979).

[2] P. H. Lim and J. M. Ozard, J. Acoust. Soc. Am. **95**, 131 (1994).

[3] P. H. Lim and J. M. Ozard, J. Acoust. Soc. Am. **95**, 138 (1994).

[4] H. Schmidt and W. A. Kuperman, J. Acoust. Soc. Am. **96**, 386 (1994).

[5] W. Munk, P. Worcester, and C. Wunsch, *Ocean Acoustic Tomography* (Cambridge University Press, Cambridge, England, 1995).

[6] F. B. Jensen, W. A. Kuperman, M. B. Porter, and H. Schmidt, *Computational Ocean Acoustics* (Springer-Verlag, New York, 2000), especially Chap. 3.

[7] A. B. Baggeroer, W. A. Kuperman, and P. N. Mikhalevsky, IEEE J. Ocean. Eng. **18**, 401 (1993).

[8] *Full Field Inversion Methods in Ocean and Seismo-Acoustics*, edited by O. Diachok, A. Caiti, P. Gerstoft, and H. Schmidt (Kluwer Academic Publishers, Dordrecht, 1995).

[9] M. B. Porter (unpublished).

[10] One may equivalently define G to be the solution to the initial value problem $G(\mathbf{x},\mathbf{x}';0)\equiv 0$, $\partial_t G(\mathbf{x},\mathbf{x}';0) = c(\mathbf{x})^2\delta(\mathbf{x}-\mathbf{x}')$. One may also define a second Green function $H(\mathbf{x},\mathbf{x}';t-t')$ through the complementary initial value problem $H(\mathbf{x},\mathbf{x}';0) = \delta(\mathbf{x}-\mathbf{x}')$, $\partial_t H(\mathbf{x},\mathbf{x}';0)\equiv 0$. There are two possible ways to define the latter through an equation similar to Eq. (2.3), depending on the boundary condition at $t-t'\to-\infty$. One may either enforce the initial condition $H=\delta(\mathbf{x}-\mathbf{x}')$ for all $t<t'$, and then release it at $t=t'$. In this case H obeys Eq. (2.3), but with $-\nabla^2\delta(\mathbf{x}-\mathbf{x}')\theta(t'-t)$, where $\theta(s)$ is the unit step function, replacing the right hand side. Alternatively, one may require $H\equiv 0$ for all $t<t'$, in which case H obeys Eq. (2.3) with $c(\mathbf{x})^{-2}\delta(\mathbf{x}-\mathbf{x}')\partial_t\delta(t-t')$ on the right hand side. One may check in either case that $H=c(\mathbf{x}')^{-2}\partial_t G$ for $t>t'$.

[11] K. V. Rao, T. M. Michaud, and H. Schmidt, OCEANS-91, IEEE Proceedings, Honolulu, HI, 779 (1991).

[12] Translation invariance occurs when the sound speed $c(\mathbf{x})$ is constant within this plane. A common example in ocean acoustic applications is the case where source and receiver move horizontally in a horizontally stratified ocean, i.e., in range-independent media where c is a function of the vertical coordinate alone.

[13] Clearly one would like $\Delta t > 2\pi/\Delta\omega$ where $\Delta\omega$ is the size of the Doppler shift to be resolved. However, one also assumes that $\Delta t \ll t_\phi$, where t_ϕ is the characteristic *dephasing time* of $S_0(t)$ beyond which the pure tone assumption breaks down.

[14] More specifically, this will occur if $v/a \lesssim \Delta\tau$, where v/a is the time scale, also entering Eq. (1.3), over which the velocity changes, and $\Delta\tau$ is a typical difference between delay times for different rays.

[15] C. M. Bender and S. A. Orszag, *Advanced Mathematical Methods for Scientists and Engineers* (McGraw-Hill, New York, 1978).

[16] It would appear that the validity of Eq. (6.3) also relies in some fashion on the fact that the ocean environment is "open," and does not confine acoustic energy in the neighborhood of the source. A closed cavitylike system, unless extremely regularly shaped, would give rise, through multiple reflections, to a chaotic acoustic signal, with a very dense three-dimensional set of wave vectors passing through each point, that would probably defy convenient decomposition.

[17] P. B. Weichman (unpublished).